

**Babeş-Bolyai University Cluj-Napoca**  
**Faculty of Environmental Science and Engineering**  
**2021**

**PhD Thesis summary**

**PLEISTOCENE DEPOSITS OF PITYUSIC ISLANDS:  
ARCHITECTURE, LUMINESCENCE CHRONOLOGY  
AND PALEOCLIMATIC IMPLICATIONS**

**Laura del Valle Villalonga**

**Supervisor: Prof. Dr. Alida Timar-Gabor**

Coastal areas are dynamic territories that are subjected to the confluence of many factors and agents that are causing transformations. These modifications and their causes can be identified from the geomorphological evidence. The study of the Pleistocene deposits of Pityusic islands can provide a very good source of information for gaining better knowledge on the history of the climate and environmental conditions, as well as the geomorphological processes that occurred during the Quaternary. In this sense, Pleistocene coastal deposits such as aeolianites, colluvial-alluvial deposits, marine deposits or palaeosols preserved along mid-latitude coastlines are used to unravel the sedimentary response of shifting shorelines to sea level change (e.g., Porat and Botha, 2008; Bateman et al., 2011) and can provide paleoclimatic records of regional and of global significance when dated precisely (El-Asmar, 1994; Kindler and Hearty, 1995; 1996; Clemmensen et al., 1997; Kindler et al., 1997; Hearty, 1998; Kocurek, 1998; Mauz, 1999; Rose et al., 1999; Sun et al., 1999; Blay and Long, 2001; Brooke, 2001; Clemmensen et al., 2001; del Valle et al., 2016; Fornós et al., 2009; Pomar et al., 2018; Roberts et al., 2012).

Over the last few years, optically stimulated luminescence (OSL) dating has become the basic tool for establishing the chronology of Quaternary siliciclastic successions all over the world and has been applied for obtaining chronological information in many environments, such as aeolian deposits (Murray and Clemmensen, 2000; Ballarini et al., 2003; Andreucci et al., 2009; Fornós et al., 2009), marine deposits (Jacobs et al., 2011; Yang et al., 2015), glacial-fluvial deposits (Shen et al., 2007; Lewis et al., 2009), lacustrine records (Armitage et al., 2007; Shen et al., 2007), reworked sand (Pomar et al., 2018), or loess (Tecsá et al., 2020a, 2020b; Constantin et al., 2021) among others. Luminescence dating techniques determine the time elapsed since the last exposure of different mineral grains to sunlight and thus are constraining the time of the burial of the sediment (Aitken, 1998). Environmental radioactivity is omnipresent in the environment and minerals such as quartz and feldspar have the ability to store the ionising radiation energy in the form of trapped charge that upon stimulation can result in a luminescence signal which can be quantified. The age is calculated by dividing the palaeodose (Gy) which is the total dose received by minerals since the last zeroing event to the environmental dose rate (Gy/ka). The development of the single-aliquot regenerative-dose (SAR) protocol for quartz for determining the radiation dose that grains received since they have been last exposed to sunlight (Murray and Wintle, 2000; 2003) has significantly increased the precision of optically stimulate luminescence chronologies.

The aeolianites are sedimentary rocks that are composed mainly of bioclastic marine sediments that have been dragged by the dynamic action of the wind from the coastal beaches where they were accumulated by the action of waves and marine currents. In the Balearic Islands this type of rock is popularly known as “mares”, and has been used since immemorial times by the inhabitants of the whole archipelago for construction (Galvañ and Ferrer, 2000). In Menorca (Pomar, 2016), Mallorca (Fornós et al., 2009; Pomar et al., 2018) or Eivissa (del Valle et al., 2016), the aeolianites contain between 1-9% detrital mineral grains, primarily quartz. The marine carbonate particles (bioclasts) were transported inland by winds from the coast or from exposed carbonate shelf areas. The quartz grains were in most cases probably related to aeolian input (Fiol et al., 2005) derived from deserts areas in North Africa (Fornós et al., 2009). Windblown sediments are considered ideal materials for the application of luminescence dating. In the last decades, optically stimulated luminescence dating was increasingly used for obtaining absolute chronologies for such sediments: western Mediterranean, Balearic Islands (Rose et al., 1999; Fornós et al., 2009), Italy, Alghero (Sardinia) (Andrecuci et al.,

2009; Pascucci et al., 2014), Liguria (Pappalardo et al., 2013), Tuscany (Mauz et al., 2013), eastern Mediterranean, Israel (Fenchen et al., 2004, Sivan and Porat, 2004), Africa, Egypt (El-Asmar and Wood, 2000), South Africa (Bateman et al., 2011, Rowell et al., 2018) or Australia, Bermuda (Hearty, 2002).

The feasibility of the application of the SAR protocol for dating aeolianites in the Balearic Islands was investigated in detail by the study carried out on samples from Eivissa by Anechietei-Deacu et al. (2018). There we have shown that the OSL signals of quartz are dominated by the fast component, the shapes of the OSL decay curves for the investigated samples being almost identical to that obtained for the calibration quartz. Preheat plateau test as well as pulse anneal, and isothermal decay experiments confirmed that signals are thermally stable. A preheat temperature of 220°C was selected based on a standard preheat test in which the 10 s preheat was applied at temperatures from 200 to 280°C in 20°C steps, whilst maintaining the cutheat at 180°C, a protocol adopted for the work carried out in this thesis as well. Dose recovery tests were carried out with satisfactory results and infrared depletion and recycling tests all resulted in excellent results with no aliquots being excluded, a trend generally followed by all samples investigated in this thesis as well. We have further shown that regardless of the grain size investigated doses up to at least 200 Gy can be accurately determined. As the dose rates for the samples of our studies typically range between 0.5 and 1 Gy/ka, this gives us confidence that ages of at least 400 ka can be accurately determined by state-of-the-art measurement procedures by using these samples, while in the case of lower dose rates such as 0.2 Gy/ka ages as high as 1 Ma could be theoretically achievable.

Shallow marine to continental Pleistocene deposits crops out quasi-continuously along the coast of the Pityusic Islands which is a tectonically stable region (Sàbat et al., 2011; Just et al., 2011). In more detail, the small archipelago of the Pityuses are composed of two large Islands; Eivissa and Formentera and sixty islets. They form the emerged part of the southern block of the Balearic promontory located in the westernmost part of the Mediterranean. Es Freus islets are separated from Formentera by a narrow and shallow passage (50 m wide, -2m deep). The lithology of Eivissa is composed mainly of folded Jurassic limestones, Cretaceous marlstone and Miocene marlstones (García de Domingo et al., 2009). Formentera is composed mainly of Miocene and Quaternary deposits. These Quaternary deposits in both islands overlie the Jurassic, Cretaceous and Miocene deposits infilling the valleys and central depressions of the islands and cover most of the coastal sections. The pleistocene sequences characterized by shallow-marine to coastal aeolian and colluvial deposits are located along cliffed coasts (del Valle et al., 2016). The section studied can be divided into; Eivissa: Cap Negret, Punta de sa Pedrera, Cala Bassa, Cala Compte and ses Salines; Es Freus: Espalmador and Formentera: Cala Sabina and Cala en Baster. All the sectors are characterized by thick aeolian deposits interbedded with colluvial deposits and palaeosols. The pleistocene sequences are delimited by an unconformity overlying the lower Miocene basement that is made up of ancient alluvial fan conglomerates or of massive lower Jurassic dolomites. Sedimentary successions containing Pleistocene coastal aeolianites at Pityusic islands display a wide sort of deposits characterized by colluvial facies and palaeosols and some shallow marine facies interbedded. The rugged geomorphology of the coasts and the basement palaeotopography contributes to the complex architecture of these deposits (Pomar et al., 2015; del Valle et al., 2016).

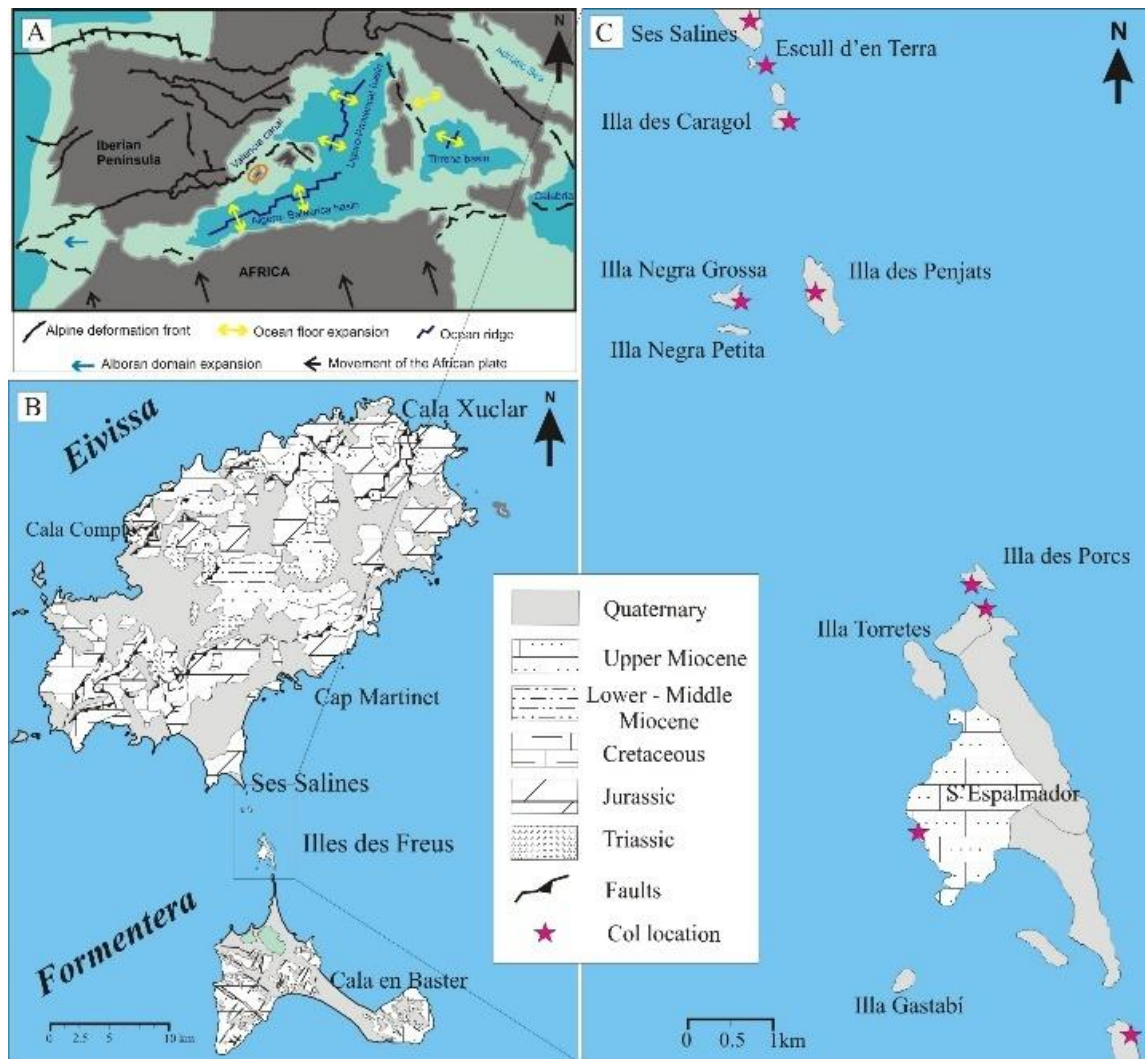


Figure 1. A) General setting of Pityusic Islands B) Geological sketch of Pityusic Islands with the location of the study site and C) Geological sketch of Es Freus Islets.

## Methods and instrumentation

We used the conventional method of lithostratigraphic logging derived by Tucker (1988). Supplementary data on cross-bed dip direction for palaeocurrent analyses was acquired, and grain size and mineralogy analyses were carried out.

One hundred and nine stratigraphical columns were measured (Fig. 4, 5 6 and 7), interpreted and correlated based on major unconformities and homogeneous units, bounding surfaces or according to the presence of continuous pedogenetic deposits. Major changes of facies vertically and laterally were taken into account. At each log major units were characterized in terms of grain size, composition and mineralogy, and discordance; as well as its arrangement or architecture, facies associations (geometry and sedimentary bodies). Both marine and continental, fossil macrofauna was collected for taxonomic identification, where possible.

Images on polished faces were obtained using an optical microscope (NATIONAL Digital Microscope), together with the binocular microscope with MOTIC Image 2.0 software and the analysis of grain size measurements was performed using the free

image analysis software IMAGEJ, allowing the measurement of the parameters of grain size (sampling of 20 grains per photo and calculation of the average of the major axis) and the determination of the composition (categories: bioclasts, lithoclasts or others). Mineralogical content was determined with a Bruker D8-Advance X-ray diffractometer, using randomly oriented powders of the bulk samples, pre-treated with H<sub>2</sub>O<sub>2</sub> to remove organic matter. The pressed powder diffraction patterns were recorded from 3° to 65° 2 $\theta$  in steps of 0.03°, 0.3-s counting time per step, at 25°C room temperature, and logged to data files for analysis. Semi-quantitative mineral analyses were based on the peak areas obtained using Diffraction EVA v.4.1 software.

The determination of the colors was carried out by comparing a sample of sediments with the Munsell Color Table ® Soil Color Chart (2000) and assigning the most similar reference code.

Twenty-nine samples in total were collected for optically stimulated luminescence OSL dating; the samples were extracted from the stratigraphic layers considered to be representative of the sequences at Cap Negret (5 samples), Punta de sa Pedrera (3 samples), Cala Bassa (3 samples), Cala Compte (4 samples), Cala en Baster (5 samples), Ses Salines (4 samples), Espalmador (5 samples) and detached under low light conditions and wrapped in very light proof material, labeled and documented.

For extracting the siliciclastic grains, primarily quartz, the inner part of each sample was extracted in the laboratory in order to be confident that the material was not exposed to sunlight and was repeatedly treated with hydrochloric acid HCl (35%) for calcium carbonate removal followed by treatment with hydrogen peroxide treatment with 30% of H<sub>2</sub>O<sub>2</sub> concentration for organic matter removal. Coarse (>63  $\mu$ m) grain fractions were separated through dry sieving. For isolating the quartz from the plagioclase feldspars and other minerals a treatment with 40% hydrofluoric acid (HF) was performed. This HF etching also removed the outer surface of the quartz grains, reducing the external ionizing alpha radiation contribution to the grains to a negligible level. Precipitated fluorides resulted after HF attack and were washed away with a 60 minutes HCl (10%) treatment.

Luminescence measurements were performed using a TL/OSL Risø DA-20 readers, equipped with an automated detection and stimulation head (DASH) (Lapp et al., 2015). Luminescence signals were detected by a PDM 9107Q-AP-TTL-03 photomultiplier. A 7.5 mm thick Hoya U-340 UV filters were used for the detection of the quartz signals. Irradiation of the samples was completed using the incorporated <sup>90</sup>Sr-<sup>90</sup>Y beta source, calibrated using gamma irradiated calibration quartz (Hansen et al., 2015). Dose rates of 0.149, 0.0943 and 0.0938 Gy/s were derived for the coarse quartz grains deposited on stainless steel disks, at the moment of measurement. Luminescence investigations were carried out using the single-aliquot regenerative dose (SAR) protocol (Murray and Wintle, 2000, 2003). Continuous wave stimulation of the luminescence signals with the blue light emitting diodes was performed for 40 s at 125 °C. The net CW-OSL signal was evaluated from the first 0.308 s of the decay curve with an early background subtraction assessed from the 1.69-2.30 s interval. A preheat temperature of 220 °C for 10 s and a cut heat to 180 °C were employed throughout the SAR protocol. The OSL response to a fixed test dose of 16 Gy was used through the whole set of measurements to correct for sensitivity changes.

At the end of each SAR cycle a high-temperature bleach for 40 s at 280 °C was performed by stimulation with the blue diodes (Murray and Wintle, 2003). The purity of

the signal from of the extracted quartz was evaluated using the infrared stimulated luminescence (IRSL) response at 60° C to a regenerative  $\beta$ -dose. A significant sensitivity to infrared stimulation accounts for an IR depletion ratio deviating more than 10% from unity (Duller, 2003). Radionuclide (Ra-226 and daughters, assumed in equilibrium with  $^{238}\text{U}$ ,  $^{232}\text{Th}$  and daughters,  $^{40}\text{K}$ ) specific activities for annual dose estimation in luminescence dating were measured by high-resolution gamma spectrometry. Dose rates were derived based on the conversion factors tabulated by Adamiec and Aitken (1998).

For the age estimation the beta attenuation and etching factor considered for 63–250  $\mu\text{m}$  fraction was  $0.900 \pm 0.060$  and also an internal dose rate of  $0.01 \pm 0.002$  Gy/ka (Vandenberghe et al., 2008). The cosmic ray component of the dose rate was calculated using the equations published by Prescott and Hutton (1994). A water content value of 3% by weight (with a relative error of 25%) was taken into account for moisture correction in age calculation. This relative average moisture value is similar to the values previously reported for other aeolianite samples from this area (i.e. Fornós et al., 2009; Del Valle et al., 2016).

## **Results**

### **Sedimentary facies and palaeosol description**

Sedimentology and stratigraphic analyses performed have allowed identifying three major facies associations and two different types of palaeosols (Fig. 2).

#### **Aeolian Facies Association**

This facies is characterised by white colour in the upper levels to very pale brown in the lower levels, well sorted fine to medium-grained bioclastic sand (125-250  $\mu\text{m}$ ), with trough cross-stratified beds laterally decrease in angle from 30° to 10°. Beds are 0.7 to 3 m thick and in the majority of the cases the upper part of these levels are partially disrupted by vertical root casts (1-6.5 cm width and 0.20 – 1 m length). Average grain composition is mainly carbonate (94%) composed of marine bioclasts with very little terrigenous material. According to X-Ray diffraction analysis, the upper aeolian levels show a high percentage of aragonite ~51% and calcite ~ 48%, followed by dolomite (5-20%). For the lower aeolian levels the predominant mineral is calcite with an average of 93-99%.

#### **Colluvial-Alluvial Facies Association**

Two levels have been described. The first is characterized by reddish silty matrix-supported breccia with angular and heterometric clasts forming layers of millimeter to centimeter thick deposits which are disrupted by calcretes levels. Some breccia layers change laterally into lens-shaped structures. The abundant subangular clasts originate from the reworked upper surface of the lower level. The mineralogical composition of the matrix is dominated by silicates (60%). These facies are interpreted as hillslope deposits.

The second is formed by subangular, cobble size sandstone filling ribbon-like channel incisions in aeolian deposits. No specific clast orientation is observed. Matrix-supported is composed of bioclastic sands with a fine to medium grain size. The mineralogical

composition is dominated by calcite (53,9%) and aragonite (46,1%). This facies is interpreted by intraformational sandstone-conglomerate channel fill.

### Shallow Marine Facies Association

This facies is characterized by massive strata (maximum thickness around 40 cm) with subrounded/rounded clasts mostly discoidal form and interstices filled by medium to coarse grained sand rich in bioclasts and marine fossils. The colour is very pale brown. The mineralogical composition is dominated by calcite (55%) and aragonite (45%).

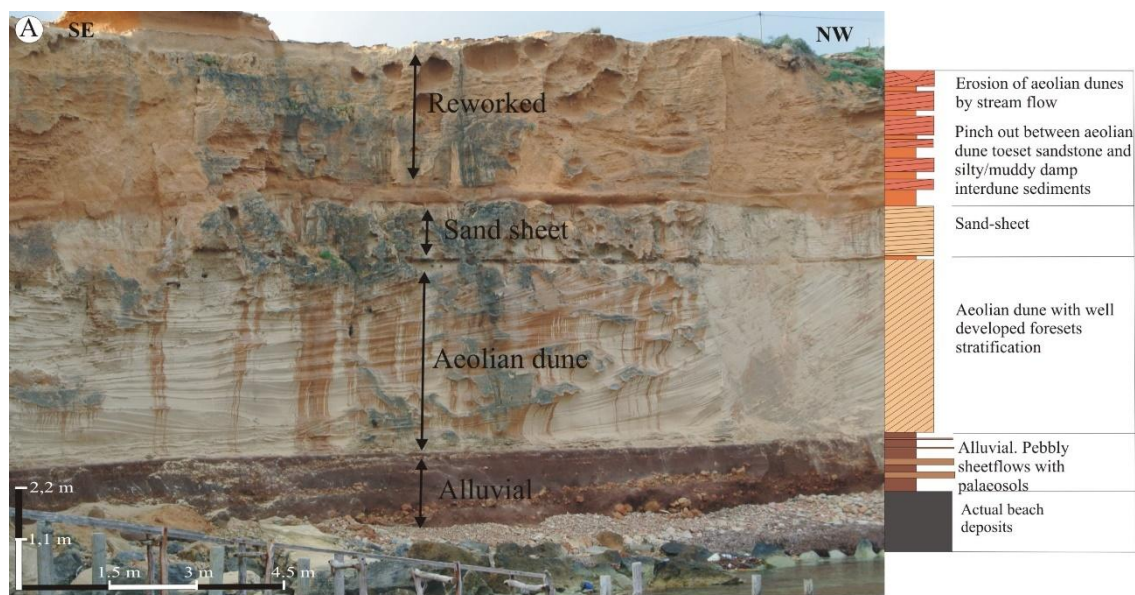


Figure 2. A) Photograph of the Pleistocene deposits of the Eastern coast of Formentera. On the right-side geological sketch with interpretation of the levels.

### Palaeosols

In general terms, two types of palaeosols are observed. The first type is characterized by massive silty-sandy texture highly bioturbated by vegetation. Its colour is very pale brown. It bears abundant terrestrial fauna (e.g. the endemic land snail *Xerocrassa ebusitana* and insect trace fossils). This sandy palaeosol shows variable thickness, changing laterally from 0.5 m to 1.5 m. In general, in the upper part, 5 cm thick calcretes are observed capping the palaeosol. The composition of the silts and sands is mainly carbonate (~80%) with calcite as major mineral (57%), followed by the aragonite with 23% and minor amounts of quartz (2%).

The second type of palaeosols are characterized by clays and silts mainly composed of reddish yellow with iron bands. Mineralogical content shows 56% clay minerals of which illite makes up 40%, 20% quartz and a minor content of calcite (11%). Calcretes have been observed locally with pisoliths horizons and abundant vegetal traces. These consist of calcified branched filamentous structures. The red mudstone palaeosol levels show variable thickness, changing laterally from 0.10 m to 0.5 m.

### OSL ages and performance of the measurement protocol



As previously reported for this region (Anechitei-Deacu et al., 2018) the quartz from the aeolianites from the Pityussic Islands displays OSL signals that are dominated by the fast component as shown by the rapid decay during optical stimulation. Also, the shape of the natural OSL signals is similar to the shape of the regenerated signals. The suitability of the samples for equivalent dose determination using the SAR protocol was tested in terms of recycling, infrared (IR) depletion and recuperation tests for each aliquot investigated. Recycling and IR depletion thresholds were set between 0.9 and 1.1. Less than 5% of the investigated aliquots had to be rejected based on these criteria. Recuperation values within 0.2% of the natural signal were exhibited by all the investigated aliquots. The equivalent doses ( $D_e$ ) were determined by projecting the sensitivity corrected natural OSL signal onto the dose response curve constructed in each case. OSL signals of these samples display a growth with dose that is best described by the sum of two saturating exponential functions.

Figure 3 presents a typical OSL decay curve and a dose response curve, depicting the good OSL properties of the investigated quartz.

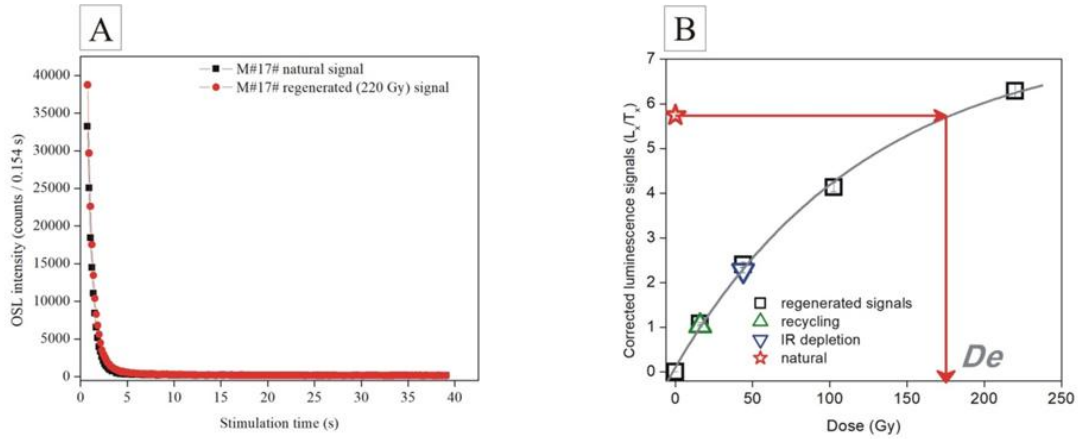


Figure 3. A) Typical decay curve of natural CW-OSL signal (black squares) in comparison to a regenerated (laboratory dose) signal (red circles). B) Representative sensitivity-corrected growth curve constructed for sample M#17# using one aliquot of coarse (63-250  $\mu\text{m}$ ) quartz grains. The regenerated doses are shown as black open squares. The sensitivity corrected natural signal is depicted as a star and the equivalent dose is indicated by arrows. Recycling and IR depletion points are represented as up and down triangles.

The ages obtained illustrate that the deposits took place from marine isotope stage MIS 6 to MIS 22 in the western coast of Eivissa, from the MIS 3 to MIS 5 in Cala Baster (north Formentera) and MIS 5d to MIS 16 in south Eivissa-Es Freus- Cala Sabina (Formentera).

It should be noted that while very high ages (at least from a conventional optically stimulated dating methodological point of view) were obtained and further discussed, this is due to the very low radioactive content of the samples and corresponding dose rate, not the equivalent dose. The equivalent doses obtained for all investigated samples are lower than 250 Gy. Anechitei-Deacu et al. (2018) presented extended dose recovery tests on quartz samples from Cala Bassa, by both delivering the artificial doses following bleaching and on top of the natural accrued dose. Their investigations confirmed that equivalent doses of such magnitude (lower than 250 Gy) should be



considered reliable, especially when using coarse ( $> 63 \mu\text{m}$ ) quartz. As far as the accuracy of the annual doses is concerned efforts were made to determine the dose rate as accurately as possible. When recording (Fig. 3) the gamma spectra counting was carried out for a very long duration of over 200 ks. In the case of these particular samples checking for radioactive disequilibrium was difficult though, due to the very low radioactivity of the material. However, we consider reasonable to assume that due to the nature of the eolianite material and its formation, radioactive equilibrium is a fair assumption. The presence of rhizoconcretions (pedodiagenetic mineral accumulations around living or dead plant roots; Klappa, 1980) in the investigated profile (Cala Bassa see figure below) is an indicator for quick cementation. Young ages were reported in literature for aeolianites at different sites, which indicate a rapid carbonate cementation after deposition.

Furthermore, for sample M#26# an intercomparison between gamma spectrometric results and beta counting measurements (Cunningham et al., 2018) was performed, the latter analysis being performed at DTU NUTECH. In the case of this particular sample, considering gamma spectrometry measurement results in a beta plus gamma dose rate of 0.258 Gy/ka while for beta counting the obtained value was 0.251 Gy/ka. Thus, the excellent agreement gives us confidence in the obtained results.

## **Stratigraphy**

Based on the main erosive surfaces and palaeosols sixteen unconformity- bounded units can be observed. Unconformities can be traced throughout the studied areas. Aeolian deposits represent the thickest and the most continuous layers in the studied area. They show a lateral shift of sedimentary facies due to the orientation of the coast at each study site, as well as due to the basement palaeotopography.

The lower unit U1 observed at Cap Negret is composed of aeolian facies with silty palaeosol layers interbedded. This palaeosol contains levels with subangular and heterometric clasts, originating from the basement. The aeolian levels represented by sand sheets and small parabolic dunes show changes laterally, being thicker seawards and thinner inland. The foresets show an average NNE dip direction, indicating that the dune migrated inland by the dominant SSW wind direction. The bed dipping angle of cross-stratified increases from  $5^\circ$  to  $15^\circ$  inland - $100^\circ/5-15\text{N}$ -. This aeolian deposit is overlying a silty palaeosol. Unit U2 outcrops in Cap Negret and Punta de sa Pedrera, with thickness decreasing in between of the two study areas. This unit is composed of aeolian facies and a silty palaeosols. At the top, unit U2 is bounded by an unconformity interpreted as colluvial. Gradual impoverishment in clast size towards upper layers indicates decreasing energy, which is reflected in the continuous upper palaeosol spreading laterally throughout the unit. The aeolian level is represented by thicker parabolic dunes that evolved to climbing dunes with active migration inland towards ENE direction. Cross-stratified layers have a higher angle upwards of  $30^\circ$  - $165^\circ/32^\circ\text{E}$  dipping SE, locally in Cap Negret angle gradually decreases to horizontal stratification. The direction of migration is oblique to the coast, and evolves to climbing dune in the cliff-front formed by the basement. The previous aeolian level in Cap Negret, reaches four meters thick in the area of sa Punta de sa Pedrera and it migrates inland perpendicular to the coast due to a relief with much less slope than in Cap Negret. The predominant average wind direction was of WSW.

Unit U3 is exposed between Cap Negret, Punta de sa Pedrera, Cala Compte and s'Espalmador. This unit is made up by two aeolian levels, facies and colluvial facies. Colluvial facies levels at the base are overlaid by aeolian facies levels resting on erosive contact. Some thin layers of travertines can be observed at the very top of the unit covering the aeolian sediments. Dune foreset bedding shows average  $040^{\circ}/25-30^{\circ}\text{SE}$  dip direction ( $25-30^{\circ}$ ) with a constant thickness in all areas. This indicates a relative change in the prevailing wind direction towards South component. In addition, differences in the migration of the dunes are observed according to the study area, so sedimentation is observed in Cala Compte during a predominant wind of the SE, due to the orientation and topography of the coast. This sedimentation does not occur on the northernmost side of Cap Negret, Punta de Sa Pedrera or in Espalmador but occurs during the period with the prevailing wind of the NW. This unit is interpreted as a parabolic dunes field migrating inland. The aeolian levels change in thickness and are separated by several palaeosol lenses. Unit U4 can be divided in two sub-units (U4a and U4b). U4a was observed in Cala Compte outcrops and is integrated by aeolian facies and the clayey palaeosol. The parallel and perpendicular view to the coast of the aeolian level shows an internal structure with a dip angle of  $030^{\circ}/20-25^{\circ}\text{SE}$ . This suggests that this dune is parabolic and migrates obliquely to the coast –SE- with a predominant direction of the NW wind.

On the other hand, sub-unit U4b is composed of the aeolian facies and of different types of palaeosols. In the upper part of the unit calcretes levels with pisoliths are observed. This unit represents a parabolic dune field migrating inland –NW- towards Cala Compte area; the cross-stratified layers have angles higher than  $30^{\circ}$  dipping NW, which gradually decrease to horizontal stratification  $5^{\circ}$  NW ( $033^{\circ}/30-35^{\circ}\text{NW}$ ). This dune indicates a predominant wind change of NW to SE. This is due to the orientation of the coast of Cala Compte towards the W-SW, only found this unit in Cala Compte. Also, the other study areas are protected by the island of Sa Conillera. Unit U5 is observed in the Cala Compte and Cap Negret outcrops. It consists of aeolian facies and different palaeosols. The aeolian levels increase in thickness towards the cliff front showing high angle cross stratification up to  $35^{\circ}$  with foreset bedding showing an average  $029^{\circ}/35^{\circ}\text{E}$  dip direction indicating a prevailing wind from NW- WNW. Levels of palaeosols with concave-up forms interbedded in the aeolian levels, possibly formed in the interdunar depressions (dune corridors), are observed. The aeolian facies in this unit present local differences, especially of the aeolian thickness, being thicker in Cala Compte and smaller in Cap Negret. This is due to the prevailing wind at the time of the formation of the dunes that was of the NW. The most obvious reason is the orientation of the coast, and the presence of the island of sa Conillera, a small island that acts as a barrier over the area of Cala Bassa and Punta de sa Pedrera from the winds of the west. It should also be noted that these areas are oriented to the north and north-east.

Unit U6 is present in the Cap Negret and Punta de Sa Pedrera outcrops and consists of sandy palaeosol and an aeolian facies. This level is represented by small parabolic dunes. Dune foreset bedding shows an average NW dip direction with an angle cross stratification of  $048^{\circ}/15 - 20^{\circ}\text{NW}$ . Additionally, the sandy palaeosol increases in thickness almost 1.5 to 2 m in Cap Negret and presents abundant carbonate nodules. The prevailing wind at this moment remained the same as in the previous unit –SE-SSE-, with some slight changes depending on the orientation and topographic features of the area, but not very noticeable. Although, there is a remobilized part of the sand from the previous features.

Unit U7 appears at Punta de sa Pedrera, at Cala Bassa and at Espalmador outcrops. It is composed by aeolian facies and a sandy palaeosol. West from Punta de sa Pedrera a palaeosol with mudcracks resting on top a level of calcretes is observed. Resting on this level there is a unit of aeolian facies represented by small superimposed parabolic dunes migrating inland (-ESE- (015°/12 - 26° E) pointing a prevailing wind direction from WNW. Between the overlying dunes there are lens-like shaped pedogenetic levels interpreted as small interdune ponds.

Unit U8 was only observed in the Cala Bassa outcrop. This unit is composed of aeolian facies and two palaeosols. The aeolian facies is interpreted as a parabolic dune migrating inland in Cala Bassa transforming to small climbing dunes inland with a migration direction of SSW. The cross-stratified layers show angles 108°/5-15°S which gradually decrease to horizontal stratification. The thickness of this level decreases as it migrated inland controlled by the presence of smooth coastal valleys or hill ridges. The main reason why one can only find these dunes with a migration inland at the coast of Cala Bassa perpendicular to the coast is due to its orientation facing a predominant wind from the N and NE. Unit U9 was observed in Cala Bassa, Cala Compte, Ses Salines, Espalmador and Cala en Baster outcrops. This unit is separated from unit U8 by an erosive unconformity. Facies architecture and succession patterns of the deposits show three clear aeolian sub-units separated by palaeosols (U9a, U9b, and U9c). The sub-unit U9a is composed of the aeolian facies and a palaeosol while sub-unit U9b is composed from the aeolian facies and the palaeosol. Sub-unit U9c is composed of facies and a sandy palaeosol. Aeolian facies represent field dunes composed of small superimposed dunes. The thickness of these deposits decreases inland and the paleocurrent analysis provides an aeolian transport to SSE, cross-stratified layers have an angle upwards 25° dipping S -085°/ 20-25°S, indicating a predominant wind direction of the NNW - NNE. Also, differences in the grain size of some levels of the dunes present in the two areas, indicates moments of greater intensity of the predominant wind of the period.

The unit U10 corresponds to a beach level located in the eastern part of Espalmador and Cala Sabina, about one meter above the current sea level. Also, to the warm and humid conditions, interdune lagoons were formed, especially in Ses Salines ( $112 \pm 8$  ka). The next unit (U11) corresponds an aeolian phase an age of  $104 \pm 9$  ka in Ses Salines, and ages of  $106 \pm 10$  ka and  $108 \pm 8$  ka obtained in Espalmador. These ages indicate its formation during the regressive substage MIS 5d. Surely this began to form during the descends of the sea level. Already in MIS 5c/b (Unit U12) palaeosols were formed in the upper part of the small parabolic dunes in s'Espalmador, es Freus, Cala Sabina and Ses Salines. On the neighboring island of Mallorca similar palaeosols have been studied, and interpreted as reflecting periods of warmer temperatures and variable conditions of aridity and vegetation cover related to periods of high-stands (Wagner et al., 2014), Cala en Baster (U12), bounded by an unconformity interpreted as an erosive surface developed during the sea level regression during the transition of MIS 5c to MIS 5b as confirmed by OSL dating ( $91 \pm 9$  ka) it is found the shallow-marine unit U13 (MIS 5a). Colluvial unit U14 (transition MIS 5 to MIS 4) rests on an unconformity level with some soft sediment structures, probably developed during a relatively minor sea level rise, or during an episode of environmental change.

The next unit U15 consists of aeolian dune deposits, present in Cala en Baster outcrops. Based on the OSL ages ( $72 \pm 7$  ka), this unit is referred to the glacial stage MIS 4. The structures and arrangement of the layers from these units indicate wind flow prevailing from the NNE-NE, which would have caused dune migration over the colluvial unit (U12). It is remarkable that the sand constitutes the thickest levels in the studied area in

volume terms. The unit U16 is divided into two subunits (U16a and U16b). Only

present in Cala en Baster is composed of aeolian sand-sheet deposits and is interpreted

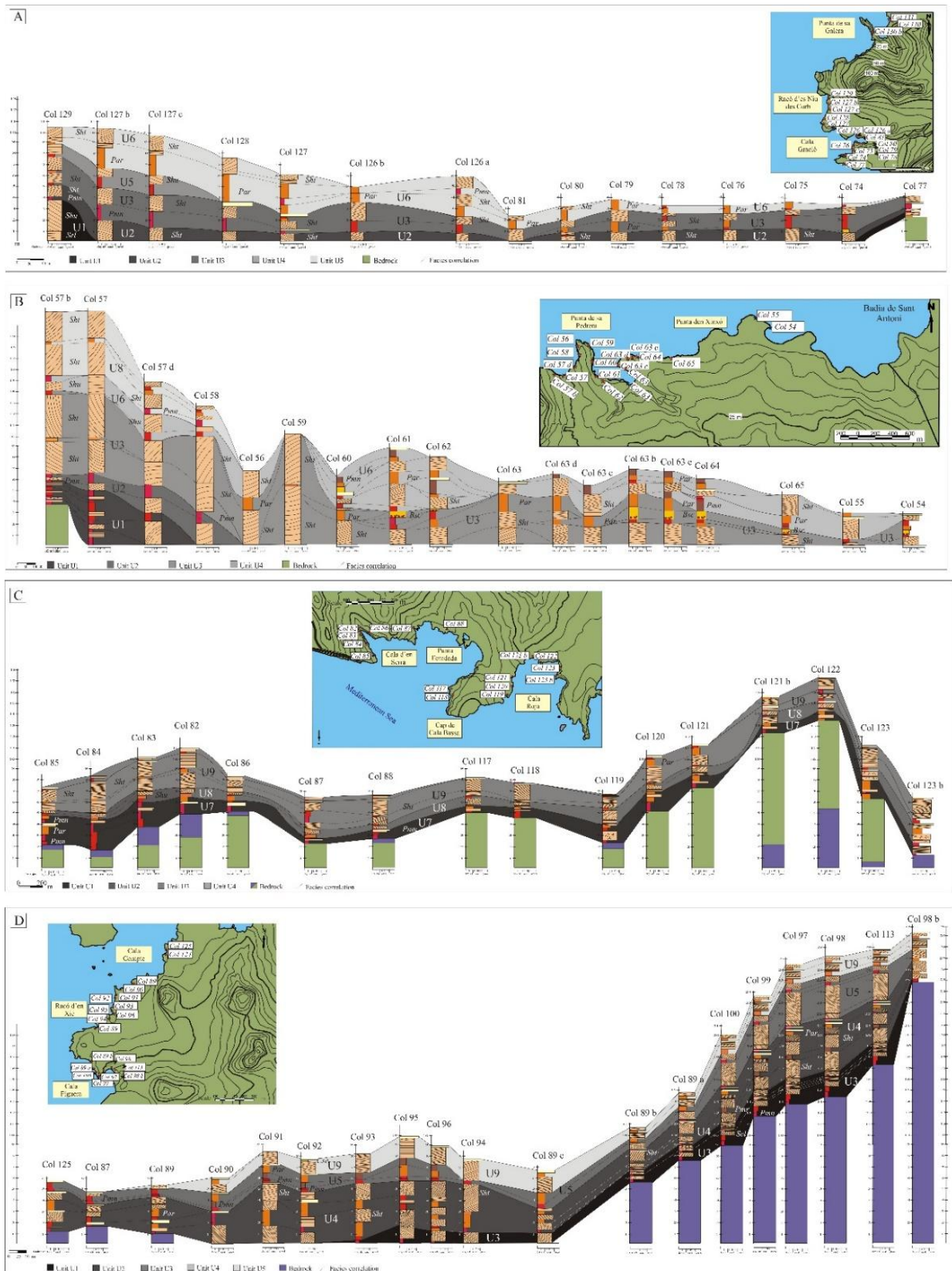
as a regressive surface developed during a minor sea level fall. Damp interdune deposits



as well as the unit thickness continuity along the Pleistocene succession indicates minor

sediment availability compared to the previous unit, the subunit U16b is a

colluvial/reworked unit present in Cala en Baster and Cala Sabina and is bounded at the base by an unconformity and at some points the sand-sheet deposits have been eroded by fluvial activity and channelized flows. Based on the OSL ages obtained on samples



from unit U16b ( $70 \pm 6$  ka and  $67 \pm 5$  ka) the unit is assigned to the transition of the glacial period MIS 4 to the interglacial MIS 3.

Figure 4. Stratigraphic logs of the outcrops studied at A) Cap Negret, B) Punta de sa Pedrera, C) Cala Bassa and D) Cala Compte.

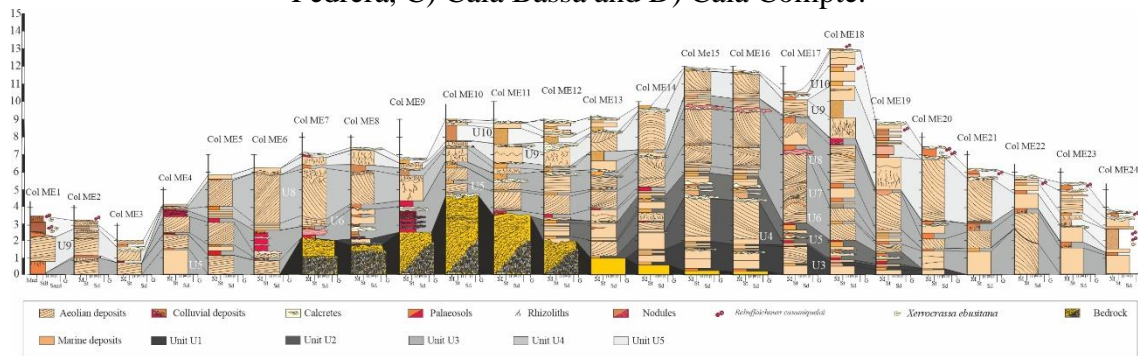


Figure 5. Stratigraphic columns of the sediments exposed at s'Espalmador (Es Freus Islets).

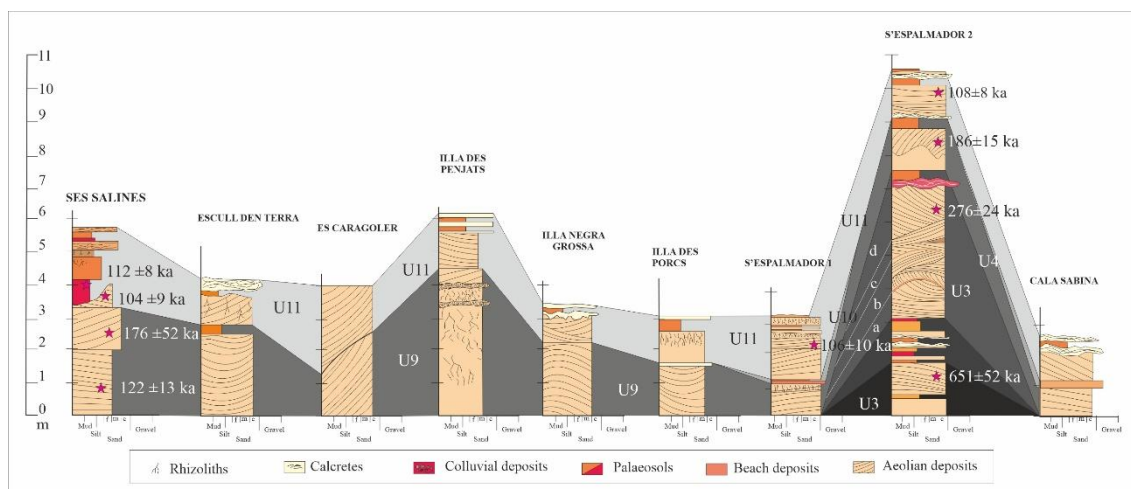


Figure 6. Stratigraphic columns of the sediments exposed at ses Salines (Eivissa), es Freus islets and Cala Sabina (Formentera).

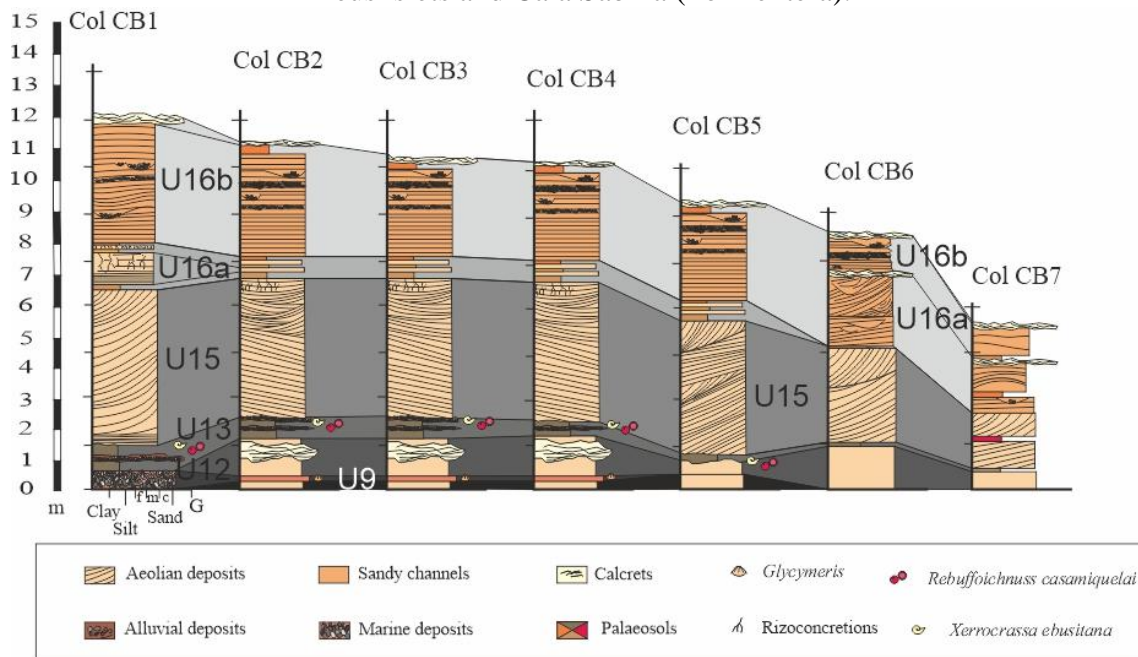


Figure 7. Stratigraphic logs of the outcrop studied at Cala en Baster, Eastern of Formentera.

## **Discussion-Climatic controls for landscape evolution and depositional evolution model**

Carbonate aeolian deposits interbedded with colluvial deposits, marine deposits and palaeosols are characteristic for the coastal Pleistocene sediments of Pityussic Islands. These successions correspond to eustatic oscillations related to glacial and interglacial periods, as well as relatively rapid warming and cooling episodes (Lowe and Walker, 2015). During interglacial periods preexisting deposits were eroded and recycled developing beach levels on narrow shore platforms cut by waves. Then, during cooling periods colluvial and alluvial deposits were formed on the coasts, besides aeolian deposits, the product of the onset of dune migration inland as sea level dropping left the continental shelf exposed (Pavelic et al., 2011; Andreucci et al., 2014). With the onset of glacial climate conditions, extensive dune fields moved to the coast on the shelf (del Valle, 2016; Pomar, 2016). The fact that changes in geomorphological processes (beach formation, fans and dune fields) that operate on the coast are conditioned by the sea level response to the availability of sediment and the existence of enough space for the development of the process that generate these fluctuations (Miall, 1996, Muto and Steel, 2000, Miall, 2010). In this way, sedimentological analyses performed on several sandstone levels have shown that the main source of these sediments is marine sands, and that the aeolianites are made up by well-sorted bioclastic sands, indicating that the source area was the coastal zone. Their mineralogical composition is predominated by calcite (>80 %).

As for the sediment composition, there is a higher presence of carbonate eskeletal fragments, molluska shell fragments, echinoderms, red algae, foraminifera, bryozoa and some lithoclasts. Furthermore, successions indicate several abrupt changes in the sediment, with silty sediments almost disappearing, leading to the accumulation of huge amounts of bioclastic sediments. These features indicate that the sediment provenance is related to the coastal zone of the continental shelf. On the other hand, temperature increase and sea level rising hamper the aeolian sediment input and greater humidity favour vegetation growth and soil formation. Thus, during warmer periods Northern wind influxes were reduced generating lower pressures formation on the Western Mediterranean which boosted warm African air masses from South (Kaspar et al., 2007; Moreno et al., 2002; Bardají et al., 2009). These African air inputs often generate dust rains which may constitute most of the Balearic soils (Fornós et al., 1997; Moreno et al., 2002; Fornós et al., 2004; Fiol et al., 2005; Muhs et al., 2010).

The coastal relief morphology, consisting of cliffs shaped on folded Lower Jurassic rocks and Miocene conglomerates together with changes in wind direction controlled the overall architecture of the sedimentary bodies. The morphology of these cliffs and the irregular position of the small catchments that reach the shoreline exert a secondary local control on sedimentation processes and thereby on the facies development and location. In addition, changes in wind patterns interact with relief and coastline orientations generating local changes in sedimentary bodies thickness and facies. These factors result in a complex architecture with large lateral variability. The architecture of the sedimentary bodies observed is interpreted as three majors sedimentary aeolian environments: climbing and cliff-front dunes, parabolic dunes and sand sheets. Therefore, the formation of the dunes is mainly controlled by the sea level (accommodation space, sediment availability), but what controls the type of dunes is the



relief (orientation of the coast, terrain rugged) interacting with the prevailing wind of the moment.

The sedimentological investigations and the OSL chronology presented allows constraining the main aeolian episodes as well as reconstructing the landscape evolution of western Eivissa between 800-900 ka and 67 ka (MIS 22 to MIS 4/3). Sixteen differentiated units indicate twelve aeolian sedimentation periods pointing out to arid environmental conditions associated to sea level dropping. These aeolian sediments are separated by palaeosols representative of warmer and relatively wetter conditions. Silty-clayey palaeosols, which in some cases have high bioturbation and reddish coloration due to rubefaction, indicate an increase in precipitations (Wagner et al., 2014). The exposure of Pleistocene deposits along the western coast punctually shows calcrete and pisoliths horizons which indicate strong aridity events (Flügel., 2014). Otherwise, the presence of travertines with laminar structures could point to the existence of water flowing conditions (Claes et al., 2015; Toker et al., 2015).

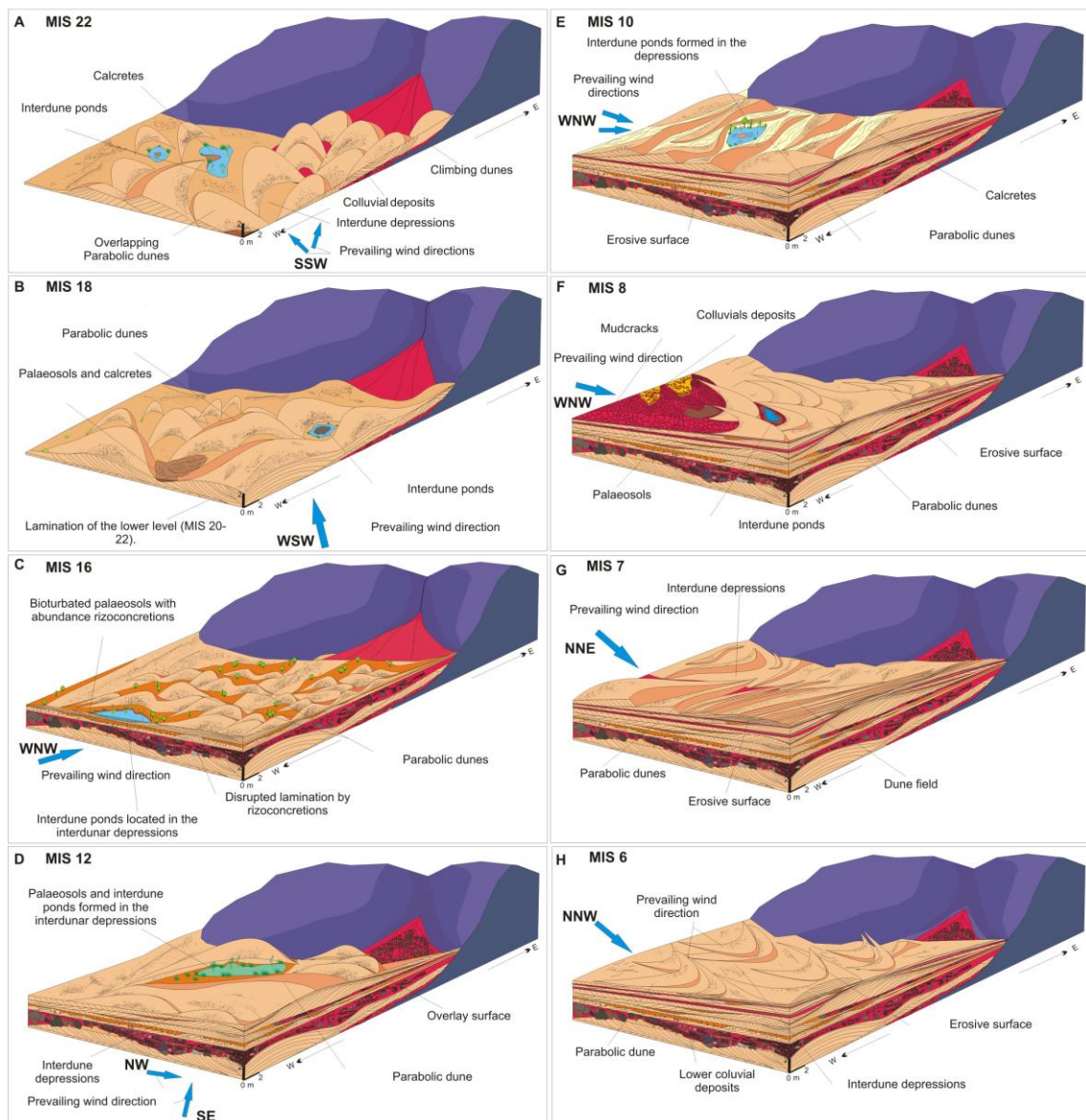




Figure 8. Depositional environment evolution model showing the succession of the main sedimentary environments and paleocurrent directions of the western coast of Eivissa from MIS 22 to MIS 6.

The first aeolian level was dated to  $754 \pm 79$  ka (MIS 22) (Fig. 8). This level corresponds to the unit U1 observed in Cap Negret and Punta de sa Pedrera outcrops. These form the coastal cliffs or the base of the Pleistocene deposits. Based on the OSL data and the error range, this level may correspond to the marine isotopic stages MIS 22 or MIS 18. During both marine stages the sea level dropped to -90 / -110 m compared to the present sea-level (Silva et al., 2009).

The second aeolian level (unit U2) presents a based on the OSL presents an age of  $747 \pm 33$  ka (M#26# Cap Negret) unit U2 is referred to the isotopic stage MIS 18. During this period, the sea level dropped to - 110 m from the current mean sea level (Silva et al., 2009). The absence of rizoconcretions is interpreted as a lack of vegetation and therefore dunes were probably formed during a very arid period.

In the different outcrops this dune level is superimposed on the previous aeolian level as well as on the basement. This sea level rising interrupted the formation of dunes and favoured the formation of soils. Some sections show palaeosols that could correspond to this moment of biostasis. On top of this pedogenetic complex small parabolic dunes can be observed sometime overlapping the mentioned soil, indicating an aeolian pulse.

Above the second dune phase lies a colluvial level with characteristic architecture of floodplain-hillslope deposits and typical forms of channelized flows. It interfingers two aeolian levels dated to  $747 \pm 33$  ka (M#36#, Cap Negret) and  $695 \pm 77$  ka (M#33#, Cap Negret), corresponding to MIS 18 and MIS 16, respectively. Thus, it is reasonable to assume that these sediments were deposited during MIS 17. This isotopic stage is characterized by a sea-level of -20 m. This scenario indicates environmental conditions changing towards a warmer and wetter climate that could correspond to an interglacial stage.

The third period of dune fields formation in the western coast of Eivissa and Espalmador (Fig. 8 and 9) is characterized by a thick aeolian level interbedded between the colluvial level described above and a palaeosol. These aeolian levels representing are parabolic dunes and belonging to unit U3 were dated to  $695 \pm 77$  ka (M#33#) (MIS 16),  $530 \pm 52$  ka (M#5# Punta de sa Pedrera), and  $651 \pm 52$  ka (#ME1# Espalmador). This isotopic stage is characterized by a progressive decreasing sea level, reaching - 130 m below present sea level (Silva et al., 2009). Lamina of the upper part of the dunes are very altered by vegetation, displaying remains of rizoconcretions that are very calcified, suggesting lesser arid conditions than for the previous dunes phases. The colluvial level represented by sheet-flood deposits within unit U3 represents the most distal part of a colluvial fan and registers scarce mass movements near the cliff foot that probably occurred after heavy rainstorms.

Changes in the environmental conditions are represented by the development of silty-clay palaeosols above the dune level. This is supported by the presence of a travertine level in the Cap Negret area and Cala Compte, which could be related to abundant water contribution and circulation, as well as to the probable increasing temperature (Claes et al., 2015; Toker et al., 2015). These factors likely ascribe these travertines and palaeosol levels to the warm period of MIS 15 or MIS 13. There is evidence that during the

transition from the glacial period MIS 16 to MIS 15, the sea level suffered a sudden rising level reaching up to about -10 m in the MIS 15 (Silva et al., 2009).

The fourth period of aeolian sedimentation observed on the western coast and in Espalmador islet (unit U4) was dated to  $464 \pm 35$  ka (M#15#, Cala Compte) and  $422 \pm 36$  ka (M#16# Cala Compte) respectively, corresponding to MIS 12. The aeolian levels observed between lower silty levels reach the largest thickness of the studied aeolian deposits. During MIS 12 a sea level dropping of -130 m occurred (Waelbroeck et al., 2002, Rohling et al., 2009, Silva et al., 2009). According to the sea level curve presented by Waelbroeck et al., (2002), during MIS 12 two regressive peaks occurred: the first peak (MIS 12a) occurred at around 460 ka and the second (MIS 12b) at 430 ka. The OSL dating results suggest that there were two periods in which there was an important aeolian sedimentation with the formation of climbing dunes of 1 to 5 m thick (unit U4) during the MIS 12. Palaeosols with a high vegetation concentration are observed in the interdune spaces. These palaeosols probably represent small ponds formed in wetter periods.

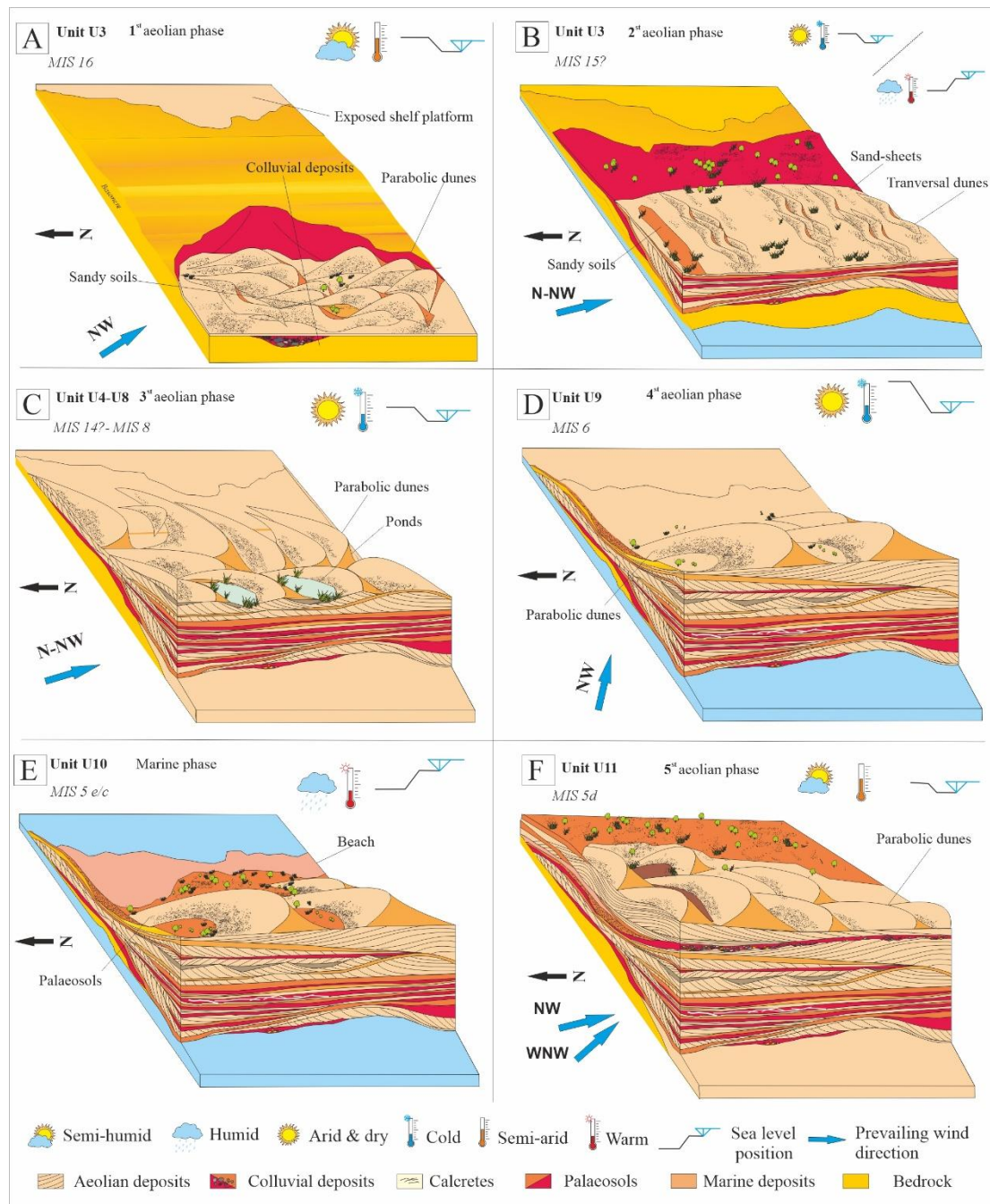


Figure 9. Depositional environment evolution model showing the succession of the main sedimentary environments and paleocurrent directions of Ses Salines- Es Freus- Cala Sabina from MIS 16 to MIS 5.

The next period of aeolian activity (unit U5) was dated to  $331 \pm 27$  ka (M#17# Cala Compte) and  $390 \pm 39$  ka (M#2# Cap Negret) and corresponds to MIS 10. This period is characterized by a low marine level of -115 m (Silva et al., 2009). This period of aeolian sedimentations reflected in the complex field of parabolic dunes that suggests a long arid period altered with short stable and humid periods represented by palaeosols. During the transition from MIS 10 to the MIS 9 there was a rapid sea-level rising reaching up to 1 m above the present sea level (Zazo, 2006). During this stable and warm period the soils proliferated. The sixth aeolian sedimentation period observed is represented by a thin aeolian level (unit U6) located above a sandy-silty level dated to  $292 \pm 29$  ka (M#3#, Cap Negret) and  $293 \pm 23$  ka (M#4# Punta de sa Pedrera), corresponding to the isotopic stage of MIS 9, probably to the regressive stage of MIS 9

b (295 ka). During the interglacial, sea level was probably close to the present levels. But in the regressive stage of MIS 9 b but sea level dropped the sea dropped about -60 m (Rohling et al., 2009; Waelbroeck et al., 2002) to -70 m (Silva et al., 2009). The seventh aeolian period is represented by a thick aeolian level, interbedded between colluvial deposits and palaeosols (unit U7) dated to of  $236 \pm 20$  ka (M#49#, Punta de sa Pedrera) and  $251 \pm 16$  ka (M#9# Cala Bassa) and  $276 \pm 24$  ka (#ME2# Espalmador). This aeolian sedimentation period corresponds to MIS 8. Studies in the phreatic speleothems of coastal caves of Mallorca, during the isotopic stage MIS 8 a sea level drop up to 23 m below the present sea level (Ginés et al., 2001). During that period parabolic superimposed dunes developed under a prevailing West wind.

The eight phase of aeolian sedimentation documented in outcrops of Cala Bassa and Cala Compte (unit U8) is represented by an aeolian level located above a silty level with an age of  $236 \pm 15$  ka (M#6# Cala Bassa), corresponding to the isotopic stage of MIS 7, and particularly to the regressive stage of MIS 7d (230 ka). At this time the sea dropped around -75 m (Waelbroeck et al., 2002, Rohling et al., 2009, Silva et al., 2009). During MIS 7, which represents a warm episode, two regressions peaks occurred (7d and 7b). According to Shackleton and Vincent (1978) and Zazo (1999), the sea level during the MIS 7 was lower than the present sea level.

The ninth aeolian activity observed on the west coast of Eivissa, Cala en Baster and Espalmador and documented here corresponds to the penultimate glacial stage MIS 6 based on obtained ages of  $172 \pm 12$  ka (M#11# Cala Bassa) and  $131 \pm 11$  ka (M#20# Cala Compte) and  $183 \pm 15$  ka (#ME3# Espalmador) (Fig. 9 and 10). This period is characterized by a low marine level (-90 m), which underwent a progressive dropping until it reached -130 m (Sidall et al., 2003, Rabineau et al., 2006, Silva et al., 2009). During this glacial stage parabolic dunes were formed. Aeolian deposits formed during the MIS 6 have been also been described in areas of the western Mediterranean, Balearic Islands (del Valle et al., 2016; 2020; Pomar et al., 2018), Sardinia (Andreucci et al., 2009) but also in the levante of the Mediterranean, concretely from the Israel coasts (Frenchen et al., 2004; Mauz et al., 2013). Unit U10 corresponds to a beach level located in the eastern part of s'Espalmador and Cala Sabina, about one meter above the current sea level. According to Butzer and Cuerda, 1962 and Nolan 1895 this beach level has the chronostratigraphic macrofauna senegalenses (*Thetystrombus latus*), this corresponds to the maximum interglacial MIS 5e. The tenth aeolian phase with an age of  $104 \pm 9$  ka in Ses Salines, and ages of  $106 \pm 10$  ka and  $108 \pm 8$  ka obtained in S'Espalmador. These ages indicate its formation during the regressive substage MIS 5d. Surely these began to form during the descens of the sea level.

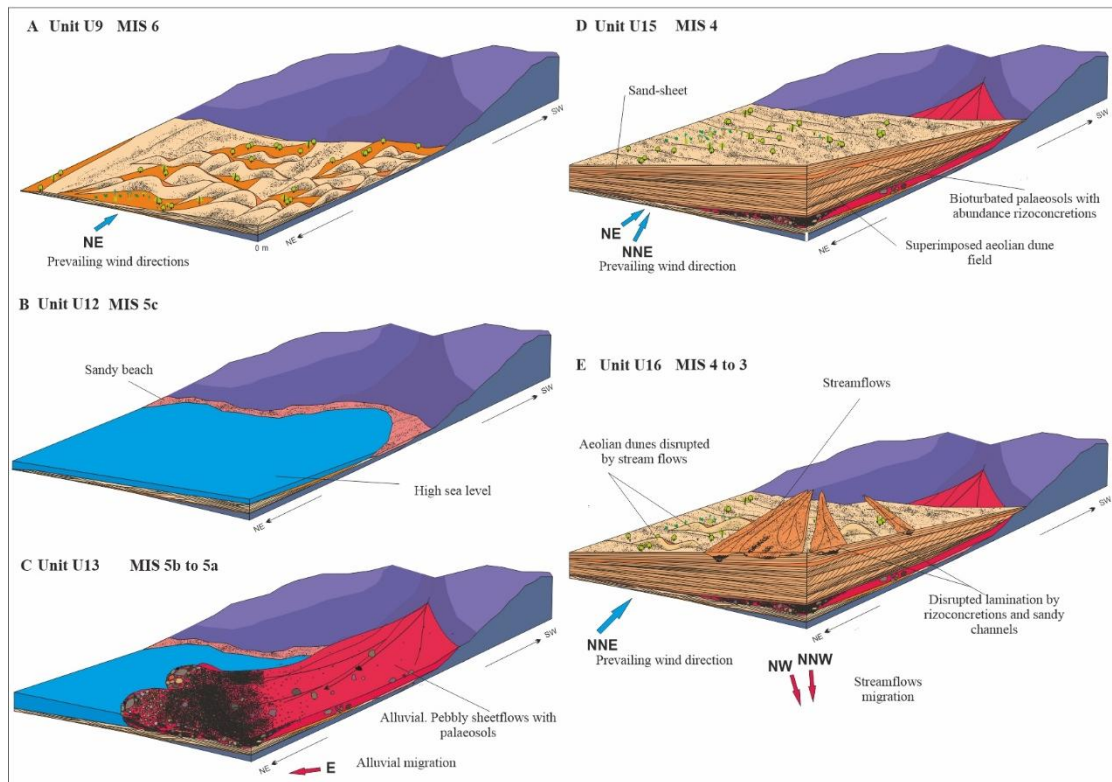


Figure 10. Depositional environment evolution model showing the succession of the main sedimentary environments, paleocurrent directions and alluvial direction migration of the Cala en Baster, Formentera from MIS 6 to MIS 4/3.

The contrary, during interglacial highstands, more precisely during MIS 5c, a beach system developed on the coastal plain, dominated by wide sandy beaches rich in macrofauna (*Glycymeris violacescens*) (U13). A variable number of highstands has been reported from the Spanish coasts during the MIS 5c, in Italy, concretely in Liguria NW (Pappalardo et al., 2013); in Tuscany Central-Western Italy (Mauz, 1999) in Sardinia, where according to Andreucci et al. (2009, 2010a, 2010b) in Alghero during the MIS 5c was dominated by progradational coastal sandy beaches systems; Tunisia (Nathan and Mauz, 2008); Israel – Carmel Coast- (Sivan and Porat, 2004) and Alexandria -NW Aegypt- (El-Asmar, 1994; El-Asmar and Wood, 2000). Over the beach level calcretes with soft-sediment structures characterized by load casts were observed, together with insect trace fossils, root casts, etc. Calcretes formed under humid and warm conditions as suggested by the existence of insect traces fossils on top, root traces in the soil. These developed in several aggrading stages. Dust and/or alluvial-colluvial deposition during arid periods alternated with carbonate leaching and precipitation form the palaeosols during more humid stages when plants, insects and bacteria played a role in calcretes formation (Huerta et al., 2015). Already in MIS 5 c palaeosols were formed in the upper part of the small parabolic dunes. On the neighbouring island of Mallorca similar palaeosols have been studied, and interpreted as reflecting periods of warmer temperatures and variable conditions of aridity and vegetation cover related to periods of sea level high-stands (Wagner et al., 2014).

During the following glacial sea level falling stages (MIS 5 b/a), alluvial - colluvial deposits developed on hillslopes and on the exposed shelf. The first alluvial unit consists mainly of silty-matrix horizontal conglomerate beds and some palaeosols on

top with subangular clasts lenses. The absence of bioclastic material suggests that this is a true alluvial unit and is indicative of the first period of fan development. These structures indicate a paleocurrent to the East. Also, during the Pleistocene, the formation of palaeosols in the western Mediterranean, as those described in U13, required warmer and relatively less arid conditions than the present conditions (Potenciano et al., 1997; Wagner et al., 2014, Paskoff and Sanlaville, 1983; Mauz et al., 2013). In this sense, Rose et al., (1999); Muhs et al., (2010) and Pomar et al., (2018) had described important pedogenetic processes during the transition of MIS 5a to MIS 4 in the neighboring island of Mallorca and the same kind of soils are present in the oriental cost of the Mediterranean (Israel) (Mauz et al., 2013).

The transition between MIS 5 to MIS 4 (ca 75 ka) is marked by a rapid sea level fall of about 70 m (below the present sea level) (Waelbroeck et al., 2002; Pascucci et al., 2014; Pomar et al., 2018). During this period an extensive dune field formed (unit U4). According with the OSL data, the thick dune field present in Cala en Baster (Unit U4, represented by sample CB3) has an age of  $72 \pm 7$  ka, corresponding to this period. Similar deposits have been described in the northern part of Ibiza (del Valle et al., 2016) as well as in Mallorca (Fornós et al., 2009) in Alicante (Brueckner, 1986); Sardinia (Andreucci et al., 2009; Pascucci et al., 2014) and the oriental coast of the Mediterranean (Sivan and Porat, 2004; Frenchen et al., 2001; 2014; Mauz et al., 2013; Nathan and Mauz, 2008). Aeolian dune fields show evidence of alternating dry periods with wind activity and the migration and accumulation of aeolian dunes, and more humid periods with water influx when the aeolian dune coexisted with palaeosols and/or lacustrine levels. The increased humidity is illustrated by the development of plant roots in the upper aeolian levels (Unit U16a). The muddy interdune deposits (damp interdunar) indicate that the water table in interdune areas was so shallow that the moist surface could capture windblown sediment. Also, after flooding and/or more humid periods, a high-water table favored the colonization of the dunes by plants leading to bioturbated horizons.

The last subunit of the outcrop (U16b) is composed by sandy channels, interpreted as stream flows. Additionally, the architecture of the unit, with abundant migrating channels, bars, erosive contacts or a complex lateral variability, indicates that this kind of features correspond to an alluvial environment. The sand grains composing sheet-flood deposits are rather similar to the aeolian ones (bioclastic) suggesting a reworking of dune sediments during ephemeral stream events, and suggest that former aeolian sands were reworked prior to lithification or during a very early stage of lithification. This could explain the preservation of the underlying aeolianites bodies with typical aeolian stratification and sediment nature and channels in between (i.e. Bateman et al., 2012; Rodríguez-López et al., 2012; Ventra et al., 2013; Pomar et al., 2018). Processes in these dynamic environments act fast. Gibbling (2006) indicates that a combination of high magnitude water flows and high sediment availability may generate both deeply incised channels and infillings. The OSL ages of this subunit (CB4-  $70 \pm 6$  ka and CB5-  $67 \pm 5$  ka) indicate its formation at the transition of MIS 4 to MIS 3. Based on the data presented, we propose that the coastal alluvial fan development in Cala en Baster and Cala Sabina is the product of the combine effects of sea level dropping that generated enough space on the coast to expose the marine sediment and blow inland the sediment (forming the dune field) and a climate cooling context that triggered temperature contrasts in the atmosphere producing episodes of intense rainfall. Thus, during the transition period (MIS 4-3; 80-60 ka) during the cold episodes the dunes moved inland on the coast covering the continental platform and the underlying alluvial deposits,



while during the relatively warmer episodes, but most likely during the transition between interstadial and stadial stages, the temperature contrasts between the sea surface temperature and the atmosphere generated suitable conditions for storms formation, discharging intense rainfall. This led to large flash floods dismantling the dunes. According to Pomar et al., (2016) this environmental context was possible because the sea level remained always below -70 m during the last glacial period.

Furthermore, deposits with the same characteristics and chronology have already been made know in the north part of Ibiza (del Valle et al., 2016) and Mallorca, were Rose and Meng., (1999) and Pomar et al., 2018 have suggested an alluviation phase for northern Mallorca at the transition from MIS 4 to MIS 3.

According to the data previously exposed, it is believed that there is a climatic correlation between the western and eastern coasts of the Mediterranean. coinciding both sedimentological and chronologically. Also, this correlation coincides with various places in the world, Morocco (Rhodes et al., 2006; El Kadiri et al., 2010); Bahamas (Carew and Mylroie, 2008) or Mexico (Ward, 1997) indicating continuous and diverse climatic fluctuations during the quaternary.

## **Conclusions**

The well dated Pleistocene successions characterized by the interference of aeolian, colluvial, alluvial and marine deposits and the intercalated paedogenetic deposits of Pityusic islands are instrumental archives for studying the influence of glacioeustatic sea level variation on coastal landscape evolution in the Mediterranean basin. These successions were correlated to temporal variations in climatic conditions that led to considerable changes in the sea level and, hence, in the accommodation space as well as the supply of sands susceptible to aeolian mobilization.

Based on the integration of the sedimentological and geomorphological studies, facies analysis and association to aeolian dunes, colluvial and marine deposits, coupled with optically stimulated luminescence dating of the Pleistocene outcrops of Pityusic Islands allowed obtaining a better understanding of the interaction between sea level and climate.

The analysis of the spatial distribution of the deposits and the erosion surfaces or contacts resulted in the identification of at least twelve periods of aeolian accumulation of marine sediments. The abundance of bioclastic material on the coastal area during the interglacial periods, while sea level was high, explains the origin of the sediments. The drop of the sea level, and the exposure of this high amount of marine sediments on the platform or exposed shelf areas resulted in accommodation space leading to the development of dunes and small cones. As such, it is concluded that arid and cold stages (glacial and subglacial stages) are represented by the development of the dune system, mainly under the action of wind.

The dune system construction followed a continuous sequence represented by the development of superimposed dunes from thinner dunes, which indicate an increase of sediment availability overtime.

In addition, the morphology of the dunes is closely linked in size and complexity to the available accommodation space. Inland space and the rugged coastal terrain were secondary constraints on dune morphology and formation.

On the contrary, the formation of colluvial deposits as well as the formation of soils, local episodes of ponds or arroyo like floodings seems to be related to wetter conditions during interglacial stages. Also, the reddish colour of the edaphic levels, which indicate a rubefaction process, points to a formation during humid and hotter periods, but the silty-sandy palaeosols indicate that their formation took place under semi-arid conditions.

The formation of calcrets corresponds to arid but still warm conditions. These indicate the alternation of short humid and arid episodes.

Optically stimulated luminescence (OSL) dating of the Pityusic deposits provided ages from MIS 22 to MIS 3, and the obtained chronology reinforced the theory that episodes of aeolian activity took place during periods when the sea level was lower.

The oldest units localized on the western coast of Eivissa in the depositional sequences consist of a series of aeolian dune fields deposits and their OSL ages is consistent with timing of the MIS 22.

The Middle Pleistocene deposits are located on the northern coast of Eivissa (e.g., Cala Xuclar, del Valle et al., 2016), western coast -Eivissa-, southern coast of Eivissa and the western part of the Espalmador islet. These sequences consist of approximately nine aeolian phases (when parabolic dunes and sand-sheet prevailed) interfered by colluvial and paedogenetic deposits, showing the alternation of warm and humid moments, with cold and arid moments represented by the dunes. The OSL chronology provided ages consistent with timing of the MIS 18 to MIS 6.

The youngest units, characterized by an extensive dune field composed mainly by parabolic dunes are localized in Cala en Baster (Formentera), Cala Xuclar (Eivissa), Ses Salines (Eivissa) and the Es Freus Islets.

This dune field underwent destructive periods characterized by flashy water influxes leading to intense reworking of the aeolian dunes and sand-sheets, the reworked bioclastic sand becoming part of the alluvial/colluvial environment. We propose that this interaction was due to periods of the transition from glacial periods (MIS 4) to the interglacial periods (MIS 3) during the Late Pleistocene, namely transition of the MIS 4/3 when thermal contrasts led to events of intense precipitation capable of generating stream-flows or flash floods dismantling partially or totally the dunes.

Periods of partial dune destruction (especially during the Late Pleistocene) are also linked to a decrease in sand availability, the development of undersaturated airflows and formation of scour surfaces, associated to an environmental change from arid to humid, with storms, causing flash floods.

On the other hand, the beach deposits observed in Cala Xuclar (del Valle et al., 2016), in Espalmador islet and Cala en Baster indicate an ancient sea level one to three meters approximately above the current sea level. The marine level is related lithologically, stratigraphically and faunistically to the warm isotopic stages MIS 5.

The prevailing wind direction analysis performed on aeolian deposits indicates that during the Lower Pleistocene, the prevailing wind direction was South, South West while during the Middle Pleistocene the prevailing wind direction was North-North-West. However, during the Late Pleistocene the prevailing wind direction was changed to North-East and South-West.

Taking into account that the study areas are all disconnected by the sea, the fact that the bedrock is totally covered by the Pleistocene deposits in this area is exceptional and suggest their continuity not only on the emerged surface and but also on submerged extensions. The age information obtained by OSL lead us to conclude that throughout the regressive phases of the sea level the Pityusic Islands and the islets of es Freus were connected by extensive dunes fields, mainly parabolic dunes that were superimposed as they migrated inland, evolving in some cases into climbing dunes or eco dunes, depending on the morphology of the basement. During interglacials these dune fields were disconnected and the formation of colluvial, paedogenetic and marine deposits predominated.

The numerical data obtained in this study supports once more the hypothesis that the Pleistocene deposits are good indicators of past climate change. If similar Pleistocene sedimentary sequences and the same highstand relationship between aeolianites formation and sea level will be found for mid-latitudes coasts of the rest of the Balearic Islands and the Mediterranean coasts, this correlation will influence the future practice of paleoclimatic research and the data could be used as input information for future predictions in marine dynamics studies that take into account climate change.

## References

- Porat, N., Botha, G., 2008. The luminescence chronology of dune development on the Maputa land coastal plain, southeast Africa. *Quaternary Science Reviews*. 27(9-10), 1024-1046.
- Bateman, M.D., Carr, A.S., Dunajko, A.C., Holmes, P.J., Roberts, D.L., McLaren, S.J., Bryant, R.G., Marker, M.E., Murray-Wallace, C.V., 2011. The evolution of coastal barrier systems: a case study of the Middle-Late Pleistocene Wilderness barriers, South Africa. *Quaternary Science Review*. 30 (1-2), 63-81.
- El-Asmar, H.M., 1994. Aeolianite sedimentation along the north western coast of Egypt: Evidence for middle to late Quaternary aridity. *Quaternary Science Reviews*. 13, 699-708.
- Kindler, P., Hearty, P.J., 1995. Pre-Sangamonian eolianites in the Bahama? New evidence from Eleuthera island. *Marine Geology*. 127, 73-86.
- Kindler, P., Hearty, P.J., 1996. Carbonate petrology as an indicator of climate and sea-level changes: new data from Bahamian Quaternary units. *Sedimentology*. 43 (2), 381-399.
- Clemmensen, L.B., Fornós, J.J., Rodríguez-Perea, A., 1997. Morphology and architecture of a Late-Pleistocene cliff-front dune, Mallorca, Western Mediterranean. *Terra Nova*. 9, 251-254.
- Kindler, P., Davaud, E., Strasser, A., 1997. Tyrrhenian coastal deposits from Sardinia (Italy): a petrographic record of high sea level and shifting climate belts during the last interglacial (isotopic substage 5e). *Palaeogeography, Palaeoclimatology, Palaeoecology*. 133, 1-25.
- Hearty, P.J., 1998. The geology of Eleuthera Island, Bahamas: a Rosetta Stone of Quaternary stratigraphy and sea-level history. *Quaternary Science Review*. 17, 333-355.

- Kocurek, G., 1998. Response of the wind system to forcing external factors: a stratigraphic view of the Saharan region. In: Alsharhan, A., Glennie, K., Whittle, G., Kendall, C. (Eds.), *Quaternary deserts and climate change*. Balkema, Rotterdam, 327-337.
- Mauz, B., 1999. Late Pleistocene records of littoral processes at the Thyrrhenian Coast (Central Italy). *Depositional environments and Luminescence chronology*. *Quaternary Science Reviews*. 18, 1173-1184.
- Rose, J., Meng, X., Watson, C., 1999. Palaeoclimate and palaeoenvironmental responses in the western Mediterranean over the last 140 ka: evidence from Mallorca, Spain; *Journal of the Geological Society*. 156, 435-448.
- Sun, J., Ding, Z., Liu, T., Rokosh, D., Rutler, N., 1999. 580.000-year environmental reconstruction from aeolian deposits at the Mu Us Desert Margin, China, *Quaternary Science Reviews*. 18, 1351-1364.
- Blay, C.T., Longman, M.W., 2001. Stratigraphy and sedimentology of Pleistocene and Holocene carbonate eolianites, Kaua'i, Hawai'i U.S.A. *Sedimentary Geology*. SEPM. 71.
- Brooke, B., 2001. The distribution of carbonate eolianite. *Earth-Science Reviews*. 55, 135-164.
- Clemmensen, L.B., Lisborg, T., Fornós, J.J., Bromley, R.G., 2001. Cliff-front aeolian and colluvial deposits, Mallorca, Western Mediterranean: a record of climatic and environmental change during the last glacial period; *Bulletin of the Geological Society of Denmark*. 48, 217-232.
- Del Valle, L., Gómez-Pujol, L., Fornós, J.J., Timar-Gabor, A., Anechitei-Deacu, V., Pomar, F., 2016. Middle to Late Pleistocene dunefields in rocky coast settings at Cala Xuclar (Eivissa, Western Mediterranean): Recognition, architecture and luminescence chronology. *Quaternary International*. 407, 4-13.
- Fornós, J.J., Clemmensen, L.B., Gómez-Pujol, L., Murray, A., 2009. Late Pleistocene carbonate aeolianites on Mallorca, Western Mediterranean: a luminescence chronology. *Quaternary Science Reviews*. 28, 2697-2709.
- Pomar, F., del Valle, L., Fornós, J.J., Gómez-Pujol, L., 2018. Late Pleistocene dune-sourced alluvial fans in coastal settings: Sedimentary facies and related processes (Mallorca, Western Mediterranean). *Sedimentary Geology*. 367, 48-68.
- Roberts, E.M., Stevens, N.J., O'Connor, P.M., Dirks, P.H.G.M., Gottfried, M.D., Clyde, W.C., Armstrong, R.A., Kemp, A.I.S., Hemming, S., 2012. Initiation of the western branch of the East African Rift coeval with the eastern branch. *Nature geoscience*. 5 (4), 289-294. Doi: 10.1038 / ngeo1432.
- Murray, A.S., Clemmensen, L.B., 2000. Luminescence dating of Holocene Aeolian sand movement. *Thy Denmark*. *Quaternary Science Reviews*. 20, 751 – 754.
- Ballarini, M., Wallinga, J., Murray, A.S., van Heteren, S., Oost, A.P., Bos, A.J.J., van Eijk, C.W.E., 2003. Optical dating of young coastal dunes on a decadal time scale. *Quaternary Science Review*. 22, 1011-1017.

- Andreucci, S., Clemmensen, L.B., Martini, A., Pascucci, V., 2009. Late Pleistocene Coastal Systems of North western Sardinia (Italy): Sandy Beaches, Coastal Dunes and Alluvial Fans. Field Trip 1. 27 th IAS Meeting. Alghero – Italy. 216, 104-116.
- Jacobs, Z., Roberts, R., Lachan, T.J., Karkanas, P., Marean, C.W., Roberts, D.L., 2011. Development of the SAR TT-OSL procedure for dating Middle Pleistocene dune and shallow marine deposits along the southern Cap coast of South Africa. *Quaternary Geochronology*. 6 (5), 491-513.
- Yang, L., Long, H., Yi, L., Wang, Y., Gao, L., Shen, J., 2015. Luminescence staining of marine sediments from the Sea of Japan using quartz OSL and polymineral pIRIR signals of fine grains. *Quaternary Geochronology*. 30 (B), 257-263.
- Shen, Z., Mauz, B., Lang, A., Bloemendal, J., Dearing, J., 2007. Optical dating of Holocene lake sediments: elimination of the feldspar component in fine silt quartz samples. *Quaternary geochronology*. 2, 150-154.
- Lewis, C.J., McDonald, E.V., Sancho, C., Peña, J.L., Rhodes, E.J., 2009. Climatic implications of correlated Upper Pleistocene glacial and fluvial deposits on Cinca and Gàññego Rivers (NE Spain) based on OSL dating and soil stratigraphy. *Global and Planetary Change*. 67 (3-4), 141-152.
- Tecsa, V., Gerasimienko, N., Veres, D., Hambach, U., Lehmkuhl, F., Schulte, P., Timar-Gabor, A., 2020a. Revisiting the chronostratigraphy of Late Pleistocene loess-palaeosol sequences in south-western Ukraine: OSL dating of Kurortne section. *Quaternary International*. 542, 65-79.
- Tecsa, V., Mason, J.A., Johnson, W.C., Miaos, X., Constantin, D., Radu, S., Magdas, D.A., Veres, D., Markovic, S.B., Timar-Gabor, A., 2020b. Latest Pleistocene to Holocene loess in the central great Plains: Optically stimulated luminescence dating and multi-proxy analysis of the Enders loess section (Nebraska, USA). *Quaternary Science Reviews*. 229, 106-130.
- Constantin, D., Mason J., Hambach, U., Veres, D., Panaiotu, C., Zeeden, C., Zhou, L., Markovic, S., Gerasimienko, N., Avram, A., Tecsa, V., Sacaciu-Groza, S.M., del Valle, L., Begy, R., Timar-Gabor, A., 2021. Accretional soil formation in northern hemisphere loess regions-evidence from OSL dating of the P/H climatic transition from China, Europe and North America. EGU 21. 2394. Doi: <https://doi.org/10.5194/egusphere-egu21-2394>.
- Adamiec, G., Aitken, M.J., 1998. Dose-rate conversion factors: update; *Ancient TL*, 16: 37- 50.
- Murray, A.S., Wintle, A.G., 2000. Luminescence dating of quartz using an improved single-aliquot regenerative-dose protocol. *Radiation Measurements*. 32, 57-73.
- Murray, A.S., Wintle, A.G., 2003. The single aliquot regenerative dose protocol: potential for improvements in reliability. *Radiation Measurements*. 37, 377-381.
- Galvañ, V.A., Ferrer, M.J., 2000. Extracción de marés. Utillaje y procedimiento. In: Graciani, A., Huerta, E., Rabasa, M., Tabales, M. *Actas del Tercer Congreso Nacional de Historia de la Construcción*. Sevilla. P. 335-341.

- Pomar, F., 2016. Arquitectura i fàcies deposicionals de la interferència entre la sedimentació al·luvial, col·luvial i eòlica a les Illes Balears durant el Pleistocè Superior: Implicacions Paleoclimàtiques. Tesi doctoral. Universitat de les Illes Balears. 375pp.
- Fiol, L.L., Fornós, J.J., Gelabert, B., Guijarro, J.A., 2005. Dust rains in Mallorca (Western Mediterranean): their occurrence and role in some recent geological processes. *Catena*. 63, 64-84.
- Pascucci, V., Sechi, D., Andreucci, S., 2014. Middle Pleistocene to Holocene coastal evolution of NW Sardinia (Mediterranean Sea, Italy). *Quaternary International*. 328-329, 3-20
- Pappalardo, M., Chelli, A., Ciampalini, A., Rellini, I., Biagioni, F., Brückner, H., Fülling, A., Firpo, M., 2013. Evolution of an Upper Pleistocene aeolianite in the northern Mediterranean (Liguria, NW Italy). *Italian Journal of Geoscience*. 132 (2), 290-303. Doi: 10.3301/ITG.2012.30.
- Mauz, B., Hijma, M.P., Amorosi, A., Porat, N., Galili, E., Bloemendal, J., 2013. Aeolian beach ridges and their significance for climate and sea level: Concept and insight from the Levant coast (East Mediterranean). *Earth-Science Reviews*. 121, 31-54. <http://dx.doi.org/10.1016/j.earscirrev.2013.03.003>.
- Frechen, M., Neber, A., Tsatskin, A., Boenigk, W., Ronen, A., 2004. Chronology of Pleistocene sedimentary cycles in the Carmel coastal plain of Israel. *Quaternary International*. 121, 41-52.
- Sivan, D., Porat, N., 2004. Evidence from luminescence for Late Pleistocene formation of calcareous aeolianite (kurkar) and paleosol (hamra) in the Carmel Coast, Israel. *Palaeogeography, Palaeoclimatology, Palaeoecology*. 211, 95-106.
- El-Asmar, H.M., Wood, P., 2000. Quaternary shoreline development: The north western coast of Egypt. *Quaternary Science Reviews*. 19, 1137-1149.
- Rowell, A., Thomas, D., Bailey, R., Stone, A., Garzanti, E., Padoan, M., 2018. Controls on sand ramp formation in southern Namibia. *Earth Surface Processes and Landforms*. 43, 150-171.
- Hearty, P., 2002. Revision of the late Pleistocene stratigraphy of Bermuda. *Sedimentary Geology*. 153, 1-21.
- Anechitei-Deacu, V., Timar-Gabor, A., Constantin, D., Trandafir-Antohei, O., del Valle, L., Fornós, J.J., Gómez-Pujol, L., Wintle, A.G., 2018. Assessing the maximum limit of SAR-OSL dating using quartz of different grain sizes. *Geochronometria*. 45 (1) 146-159.
- Sàbat, F., Gelabert, B., Rodríguez-Perea, A., Jiménez, J., 2011. Geological structure and evolution of Majorca: implications for the origin of the western Mediterranean; Tectonophysics. 510, 217-238.
- Just, J., Hübscher, C., Betzler, C., Lüdmann, T., Reicherter, K., 2011. Erosion of continental margins in the Western Mediterranean due to sea-level stagnancy during the Messinian salinity crisis. *Geo-Marine Letters*. 31, 51-64.
- García de Domingo, A., Díaz de Neira, J.A., Gil-Gil, J., Cabra-Gil, P., 2009. Cartografía y Memoria del Mapa Geológico de España a escala 1:25.000 (Plan MAGNA, 2ª serie)



de la Hoja 799 I (Santa Eulària des Riu). Madrid, Servicio de Publicaciones del IGME. 77 p. Col·lecció 2<sup>a</sup> Sèrie.

Pomar, F., Del Valle, L., Fornós, J.J., Gómez-Pujol, L., 2015. Registro sedimentario litoral del Pleistoceno en las Islas Baleares (Mediterráneo occidental): implicaciones paleoclimáticas. VIII Jornadas de Geomorfología Litoral. GeoTemas 15, 65-68.

Tucker, M., 1988. Techniques in Sedimentology. Blackwell Scientific Publications, Oxford, p. 394.

Munsell Color (Firm). Munsell Soil Color Charts: With Genuine Munsell Color Chips. Grand Rapids, MI: Munsell Color, 2010. Available online: <https://search.library.wisc.edu/catalog/9910109259802121/cite> (accessed on 17 November 2018).

Lapp, T., Kook, M., Murray, A.S., Thomsen, K., Buylaert, J.P., Jain, M., 2015. A new Luminescence Detection and Stimulation Head for the Risø TL/OSL reader. Radiation Measurements. 81, 178-184.

Hansen, V., Murray, A., Buylaert, J-P., Yeo, E-Y., Thomsen, C., 2015. A new irradiated quartz for beta source calibration. Radiation Measurements. 81, 123-127.

Duller, GAT., 2003. Distinguishing quartz and feldspar in single grain luminescence measurements. Radiation Measurements. 37, 161-165.

Vandenbergh D.A.G, De Corte F, Buylaert J-P, Kučera J and Van den haute P., 2008. On the internal radioactivity in quartz. Radiation Measurements. 43,771-775

Prescott, J.R., Hutton, J.T., 1994. Cosmic ray contributions to dose rates for luminescence and ESR dating: Large depths and long terms variations. Radiation Measurements. 23 (2-3), 497-500.

Klappa, C.F., 1980. Rhizolits in terrestrial carbonates: classification, recognition, genesis and significance. Sedimentology. 27, 613-629.

Cunningham, A.C., Murray, A.S., Armitage, S., Autzen, M., 2018. High-precision natural dose rate estimates through beta counting. Radiation Measurements. 120, 209-214

Lowe, J.J., Walker, M.J.C., 2015. Reconstructing Quaternary Environments. Routledge. 538 pp.

Pavelic, D., Kovacic, M., Vlahovic, I., Wacha, L., 2011. Pleistocene calcareous aeolian-alluvial deposition in a steep relief karstic coastal belt (island of Hvar, eastern Adriatic, Croatia). Sedimentary Geology. 239, 64-79

Andreucci, S., Panzeri, L., Martini, P., Maspero, F., Martini, M., Pascucci, V., 2014. Evolution and architecture of a West Mediterranean Upper Pleistocene to Holocene coastal apron-fan system. Sedimentology. 61, 333-361

Miall, A.D., 1996. The Geology of Fluvial deposits. Sedimentary Facies, Basin Analysis, and Petroleum Geology. Springer: 582

Muto, T., Steel, R.J., 2000. The accommodation concept in sequence stratigraphy: some dimensional problems and possible redefinition. Sedimentary Geology, 130: 1-10.  
Nielsen, K.A., Clemmensen, L.B., Fornós, J.J., 2004. Middle Pleistocene magnetostratigraphy and susceptibility stratigraphy: data from a carbonate aeolian

- system, Mallorca, Western Mediterranean; *Quaternary Science Reviews*. 23, 1733-1756.
- Miall, A.D., 2010. *The Geology of Stratigraphic Sequences*. Springer-Verlag. Berlin Heidelberg. 2a Edició: 522
- Moreno, A., Cacho, I., Canals, M., Prins, M.A., Sanchez-Goñi, M.F., Grimalt, J.O., Weltje, G.L., 2002. Saharan dust transport and high-latitude glacial climatic variability: the Alboran Sea record. *Quaternary Research*. 58, 318-328
- Bardají, T., Goy, J.L., Zazo, C., Hillaire-Marcel, C., Dabrio, C.J., Cabero, A., Ghaleb, B., Silva, P.G., Lario, J., 2009. Sea level and climate changes during OIS 5e in the Western Mediterranean. *Geomorphology*. 104, 22-37.
- Kaspar, F., Spanghehl, T., Cubasch, U., 2007. Northern Hemisphere winter storm tracks of the Eemian interglacial and the last glacial inception. *Climate of the past*. 3, 181-192
- Muhs, D.R., Budahn, J., Avila, A., Skipp, G., Freeman, J., Patterson, D., 2010. The role of African dust in the formation of Quaternary soils on Mallorca, Spain and implications for the genesis of Red Mediterranean soils. *Quaternary Science Reviews*. 29, 2518-2543.
- Wagner, S., Eckmeier, E., Skowronek, A., and Günster, N., 2014. Quaternary paleosols and sediments on the Balearic Islands as indicators of climate changes. *Catena*. 112, 112-124.
- Flügel, E., 2014. *Microfacies of Carbonate Rocks. Analysis, Interpretation and Application*. Springer. Berlin, 976 p.
- Claes, H., Soete, J., Van Noten, K., El Desouky, H., Marques-Erthal, M., Vanhaecke, F., Özkul, M., Swennen, R., 2015. Sedimentology, three-dimensional geobody reconstruction and carbon dioxide origin of Pleistocene travertine deposits in the Ballık area (South-west Turkey). *Sedimentology*. 62 (5), 1408-1445.
- Toker, E., Kayseri-Özer, M.S., Özkul, M., Kele, S., 2015. Depositional system and palaeoclimatic interpretations of Middle to Late Pleistocene travertines: Kocabaş, Denizli, south-west Turkey. 62 (5), 1360-1383.
- Silva, P.G., Zazo, C., Bardají, T., Baena, J., Lario, J., Rosas, A., Van der Made, J., 2009. Tabla cronostratigràfica del Cuaternario de la Península Ibérica, v.2. AEQUA. Available at: [www.aequa.es](http://www.aequa.es)
- Waelbroeck, C., Labeyrie, L., Michel, E., Duplessy, J.C., Mcmanus, J.F., Lambeck, K., Balbon, E., Labracherie, M., 2002. Sea-level and deep water temperature change derived from benthic foraminifera isotopic records; *Quaternary Science Reviews*. 21, 295-305.
- Rohling, E.J., Grant, K., Bolshaw, M., Roberts, A.P., Siddall, M., Hemleben, C., Kucera, M., 2009. Antarctic temperature and global sea level closely coupled over the past five glacial cycles; *Nature Geoscience*. 2, 500–504.
- Zazo, C., 2006. Cambio Climático y nivel del mar: La península Ibérica en el contexto Global. *Rev. C & G*. 20 (3-4), 115-130.
- Ginés, J., Fornós, J.J., Ginés, A., Gràcia, F., Delita-la, C., Taddeucci, A., Tuccimei, P., Vesica, P.L., 2001. Els espeleotemes freàtics de les coves litorals de Mallorca: canvis

- del nivel de la Mediterrània i paleoclima en el Pleistocè superior. In: Pons, G.X., Guijarro, J.A. (Eds): El canvi climàtic: passat, present i futur. Palma de Mallorca. Monografies de la Societat d'Història Natural de les Balears. 9, 33-52.
- Shackleton, N.J., Vincent, E., 1978. Oxygen and carbon isotope studies in recent foraminifera from the southwest Indian Ocean. *Marine Micropaleontology*. 3, 1-13.
- Zazo, C., 1999. Interglacial sea levels. *Quaternary International*. 55, 101-113.
- Sidall, M., Rohling, E.J., Almogi-Labin, A., Hemleben, C.H., Melscher, D., Schmelzer, I., Smed, D.A., 2003. Sea-level fluctuations during the last glacial cycle. *Nature*. 423, 853-858.
- Rabineau, M., Berné, S., Olivet, J.L., Aslanian, D., Guillocheau, F., Joseph, P., 2006. Paleo sea levels reconsidered from direct observation of paleoshoreline position during Glacial Maxima (for the last 500,000 yr). *Earth and Planetary Science Letters*. 252, 119-137.
- Del Valle, L., Pomar, F., Fornós, J.J., Gómez-Pujol, L., Timar-Gabor, A., 2020. Lower to Middle Pleistocene coastal dune fields formation in the western Mediterranean (Western Eivissa, Balearic archipelago): Chronology and landscape evolution. *Aeolian Research*. 45, 1-16. Doi: <https://doi.org/10.1016/j.aeolia.2020.100595>.
- Butzer, K. W., Cuerda, J., 1962. Nuevos yacimientos cuaternarios de las Baleares. *Notas y Comunicaciones Instituto Geológico y Minero de España*. 67, 25-70.
- Nolan, H., 1895. Structure géologique d'ensemble de l'archipel Baléare. *Bull. Soc. Geol. France*. 3, 76-91.
- Nathan, R.P., Mauz, B., 2008. On the dose-rate estimate of carbonate-rich sediments for trapped charge d Sivan, D., Porat, N. 2004. Evidence from luminescence for Late Pleistocene formation of calcareous aeolianite (kurkar) and paleosol (hamra) in the Carmel Coast, Israel. *Palaeogeography, Palaeoclimatology, Palaeoecology*. 211, 95-106.
- Huerta, P., Rodríguez-Berriguete, A., Martín-García, R., Martín-Perez, A., La Iglesia Fernández, A., Alonso-Zarza, A.M., 2015. The role of climate and aeolian dust input in calcrete formation in volcanic islands (Lanzarote and Fuerteventura, Spain). *Palaeogeography, Palaeoclimatology, Palaeoecology*. 417, 66-79.
- Potenciano, A., Espejo, R., Garzón, G., 1997. Caracterización y ambiente de formación de los paleosuelos rojos en la cuenca terciaria del río Amarguillo (Toledo). *Geogaceta*. 22, 157-160.
- Paskoff, R., Sanlaville, P., 1983. Les côtes de la Tunisie: Variations du Niveau Marin depuis le Tyrrhenien. Editions Maison de l'Orient, Lyon, France. 192 pp.
- Bateman, M.D., Bryant, R.G., Foster, I.D.L., Livignstone, I., Parsons, A.J., 2012. On the formation of sand ramps: A case study from Mojave Desert. *Geomorphology*. 161-162, 93-109.
- Rodríguez-López, J.P., Liesa, C.L., Van Dam, J., Lafuente, P., Arlegui, L., Ezquerro, L., De Boer, P.L., 2012. Aeolian construction and alluvial dismantling of a fault-bounded intracontinental perspective on Late Pliocene climate change and variability. *Sedimentology*. 59, 1536-1567.

Ventra, D., Chong, G., De Boer P.L., 2013. Colluvial sedimentation in a hyperarid setting (Atacama Desert, northern Chile): Geomorphic controls and stratigraphic facies variability. *Sedimentology*. 60, 1257-1290.

Gibbling, M.R., 2006. Width and Thickness of Fluvial Channel Bodies and Valley Fills in the Geological Record: A Literature Compilation and classification. *Journal of Sedimentary Research*. 76, 731-770.

Rhodes, E.J., Singarayer, J.S., Raynal, J.P., Westaway, K.E., Sbihi-Alaoui, F.Z., 2006. New age estimates for the Palaeolithic assemblages and Pleistocene succession of Casablanca, Morocco. *Quaternary Science Reviews*. 25, 2569-2585.

El Kadiri, K., Sanz de Galdeano, C., Pedrera, A., Chalouan, A., Galindo-Zaldívar, J., Julià, R., Akil, M., Hlila, R. Ahmamou, M., 2010. Eustatic and tectonic control on Quaternary Ras Leona marine terraces (Strait of Gibraltar, northern Morocco). *Quaternary Research*. 74 (2), 277-288. DOI: <http://doi.org/10.1016/j.yqres.2010.06.008>

Carew, J.L., Mylroie, J.E., 2008. Quaternary carbonate eolianites of the Bahamas: Useful analogues for the interpretation of ancient rocks? In: Abegg, F.E., Harris, P.M., Loope, D.B., (Eds.). *Modern and ancient carbonate eolianites SEPM Special Publication*. 71, 33-45.

Ward, W.C., 1997. Geology of coastal islands, north eastern Yucatan Peninsula. In: Vacher, H.L., Quinn, L. (Eds.). *Geology and Hydrogeology of carbonate islands. Developments in Sedimentology*, 54. Elsevier Science B.V. Publishers, pp. 275-298.

## Publications:

1. del valle Villalonga, L., Timar-Gabor, A., Fornos, J., 2019. Geomorphological Processes and Environmental Interpretation at Espalmador islet (Western Mediterranean). *Journal of Marine Science and Engineering*, 7, 5, 144.  
<https://doi.org/10.3390/jmse7050144>
2. del valle Villalonga, L., Pomar, F., Fornos, J., Gomez-Pujol, L., Timar-Gabor, A., 2020. Lower to middle pleistocene coastal dune fields formation in the western mediterranean (Western Eivissa, Balearic archipelago): Chronology and landscape evolution. *Aeolian research*, 45, 100595.  
<https://www.sciencedirect.com/science/article/abs/pii/S187596372030046X?via%3Dihub>
3. del Valle, L., Fornós, J.J., Pomar, F., Pons, G.X., Timar-Gabor, A., 2020. Aeolian-Alluvial interactions at Formentera (Balearic islands, western Mediterranean): The late pleistocene evolution of a costal system. *Quaternary International*, 566-567, 271-283.  
<https://www.sciencedirect.com/science/article/abs/pii/S1040618220302433>
4. del Valle, L., Timar-Gabor, A., Fornós, J.J., Pons, G.X., 2020. Lower to Upper Pleistocene Coastal Deposits from the Ses Salines, Es Freus Islets and Cala Sabina (Pityusic Islands, Western Mediterranean): Chronology and Evolution. *Journal of Coastal Research* 95 (sp1), 448-452.  
<https://bioone.org/journals/journal-of-coastal-research/volume-95/issue-sp1/SI95-087.1/Lower-to-Upper-Pleistocene-Coastal-Deposits-from-the-Ses-Salines/10.2112/SI95-087.1.short>

Works submitted to national or international conferences 2018-2021.

1. Title of the work: Lower to Upper Pleistocene Coastal Deposits from the Ses Salines, Es Freus Islets and Cala Sabina (Pityusic Islands, Western

- Mediterranean): Chronology and Evolution. Name of the conference: *International Coastal Symposium*. Type of event: Conference. Geographical area: International. Type of participation: 'Participatory - poster City of event: Sevilla, Spain Date of event: 2021. Organizing entity: Universidad Pablo de Olavide. Authors: Laura del Valle; Alida Timar-Gabor; Joan J. Fornós; Guillem X. Pons. "Journal of Coastal Research".
2. Title of the work: Lower to Middle Pleistocene coastal deposits from western Eivissa (Western Mediterranean): chronology and evolution. Name of the conference: *EGU General Assembly*, 7-12 april 2019. Type of event: Conference. Geographical area: International. Type of participation: Participatory - Poster communication. City of event: Viena, Austria. Date of event: 2019. Organising entity: European Geosciences Union. Authors: del Valle, L.; Pomar, F.; Fornós, J.J.; Timar-Gabor, A.
  3. Title of the work: Conos aluviales alimentados por campos dunares costeros durante el Pleistoceno en la zona d Cala en Baster (Formentera, Mediterráneo occidental). Name of the conference: *XV REUNIÓN NACIONAL CUATERNARIO* Type of event: Conference. Type of participation: Participatory - oral communication. City of event: Bilbao, Spain Date of event: 2019. Organising entity: 07895 - Unidad de Formación e Investigación en Cuaternario de la UPV/EHU. Authors: del Valle, L.; Fornós, J.J.; Pomar, F.; Pons, G.X."Libro de Resúmenes. XV Reunión Nacional de Cuaternario. ISBN 978-84-17713-16-4. D.L. SS 693-2019.)".
  4. Title of the work: Descripción e interpretación ambiental del Pleistoceno Litoral de Cala en Baster (Formentera, Mediterráneo occidental): procesos geomorfológicos. Name of the conference: *X Jornadas de Geomorfología Litoral*, Castelldefels, 4 a 6 de septiembre de 2019. Type of event: Conference. Type of participation: oral communication. City of event: Castelldefels (Barcelona), Spain Date of event: 2019. Organising entity: Institut de Ciències del Mar (ICM-CSIC). Authors: del Valle, L.; Timar-Gabor, A.; Fornós, J.J.; Pons, G.X."Durán R., Guillén J., Simarro G. (eds) X Jornadas de Geomorfología Litoral, Libro de Ponencias. Castelldefels, 4 a 6 de septiembre de 2019. 292 pp.".
  5. Title of the work: Late Pleistocene coastal deposits of south-western Formentera (Western Mediterranean): Chronology, landscape and climatic variability. Name of the conference: *34th IAS International Meeting of Sedimentology*, Roma 10-13 September 2019. Type of event: Conference. Geographical area: International Type of participation: 'Participatory – poster. City of event: Roma, Italy Date of event: 2019. Organising entity: Università degli Studi di Roma - La Sapienza (UNIROMA). Authors: del Valle, L.; Timar-Gabor, A.; Fornós, J.J.
  6. Title of the work: Lower to Late Pleistocene coastal deposits of Eivissa (Western Mediterranean): chronology and evolution. Name of the conference: *VII Jornades de Medi Ambient de les Illes Balears*. Mallorca, Eivissa i Menorca Type of event: Conference Type of participation: Participatory - oral communication. City of event: Eivissa, Spain Date of event: 2018 Organising entity: Societat d'Història Natural de les Balears. Authors: del Valle, L.; Pomar, F.; Fornós, J.J.; Gómez-Pujol, Ll., Timar-Gabor, A."VII Jornades de Medi Ambient de les Illes Balears. Mallorca, Eivissa i Menorca. Ponències i resums".

7. Title of the work: Jaciments litorals del Quaternari: aproximació a un inventari de les Gimnèsies i de les Pitiüses Name of the conference: *VII Jornades de Medi Ambient de les Illes Balears* Type of event: Conference. Type of participation: Participatory - oral communication City of event: Spain Date of event: 2018. Organising entity: Societat d'Història Natural de les Balears. Authors: Vicens, D.; del Valle, L.; Pons, G.X. "In: Pons, G.X., del Valle, L., Vicens, D., Pinya, S., McMinn, M i Pomar, F. (eds.) 2018. Llibre de ponències i resums de les VII Jornades de Medi Ambient de les Illes Balears. Societat d'Història Natural de les Balears (SHNB) - Universitat de les Illes Balears (UIB), Palma."